SKB

TECHNICAL REPORT 94-10

Project Caesium–An ion exchange model for the prediction of distribution coefficients of caesium in bentonite

Hans Wanner[1], Yngve Albinsson[2], Erich Wieland[1]

1 MBT Umwelttechnik AG, Zürich, Switzerland
2 Chalmers University of Technology, Gothenburg, Sweden

June 1994

SVENSK KÄRNBRÄNSLEHANTERING AB
SWEDISH NUCLEAR FUEL AND WASTE MANAGEMENT CO
BOX 5864 S-102 40 STOCKHOLM
TEL. 08-665 28 00 TELEX 13108 SKB S
TELEFAX 08-661 57 19

PROJECT CAESIUM - AN ION EXCHANGE MODEL FOR THE PREDICTION OF DISTRIBUTION COEFFICIENTS OF CAESIUM IN BENTONITE

Hans Wanner[1], Yngve Albinsson[2], Erich Wieland[1]

1 MBT Umwelttechnik AG, Zürich, Switzerland
2 Chalmers University of Technology, Gothenburg, Sweden

June 1994

Swedish Nuclear Fuel and Waste Management Co. (SKB)

Project Caesium

An ion exchange model for the prediction of distribution coefficients of caesium in bentonite.

Hans Wanner[1]), Yngve Albinsson[2]) and Erich Wieland[1])

[1]) MBT Umwelttechnik AG, Zürich, Switzerland
[2]) Chalmers University of Technology, Gothenburg, Sweden

June 1994

Abstract

A surface chemical model is established to thermodynamically describe caesium sorption on bentonite. Caesium sorption is studied on Wyoming bentonite MX-80 in solutions of NaCl, KCl, $MgCl_2$, $CaCl_2$, $NaNO_3$ and $Ca(NO_3)_2$ of concentrations varying between 0.025M and 1M, as well as in the weakly saline Allard groundwater and the strongly saline Äspö groundwater. Based on these experiments it is shown that the sorption behaviour of caesium on bentonite can be described, within the experimental and model uncertainties, in terms of a one-site ion exchange model. The ion exchange constant for the replacement of Na^+ on montmorillonite by Cs^+ is $\log K_{ex}^\circ = 1.6$. The model predictions compare well with sorption data published in the open literature on both Wyoming bentonite MX-80 and other types of bentonite.

For the analysis of diffusion experiments in compacted bentonite, the apparent diffusivity of tritiated water, HTO, is used as an analogue to estimate the pore diffusivity of Cs^+. Since insufficient information is available at present to estimate the porosity actually available for diffusion in compacted bentonite, it is assumed that the diffusion porosity can be approximated by using the value of the bulk porosity. Under these circumstances, the cation exchange capacity (CEC) found to be available for the diffusing species in compacted bentonite corresponds to about 12% of the total CEC of bentonite. It is recognised that the errors made in the estimation of the pore diffusivity and of the diffusion porosity are contained in the reduction factor of the CEC. A discussion of the factors affecting the diffusivities of radionuclides and the problem of establishing consistent sets of diffusivity data is given in the Appendix.

Table of Contents

1 Introduction

The analysis of the distribution coefficients of hazardous materials between the transport media and the stationary phase is of primary importance for the understanding and prediction of the retardation processes along a migration path. The physico-chemical reactions a dissolved species can undergo with the stationary phase are numerous. They include physical adsorption based on electrostatic attraction, and chemical adsorption such as ion exchange and surface complexation. These are reactions that take place on the surface of the stationary phase. There are other retardation processes which may be of importance under certain conditions, such as precipitation, coprecipitation, matrix diffusion, molecular filtration or mineralisation. However, for the migration of most actinides and fission products, surface reactions are expected to be the main contributor to retardation. Therefore, it is of crucial importance to have a reliable tool for the prediction of these reactions in a natural environment.

The understanding of the surface reactions of actinides and fission products in clays will provide a reliable basis for predicting their migration behaviour and deriving site-specific K_d values. Due to their thermodynamic basis, surface reaction models can predict sorption for any type of groundwater composition and many types of bentonite. Their application can most probably be extended to crystalline rock, in which the water-bearing fractures are lined with weathered material whose surfaces may have clay-like properties.

The aim of this report is to provide a quantitative and applicable basis for ion exchange modelling in clays. Caesium is taken as a reference element, and its K_d values obtained from both batch and diffusion experiments are explained and independently predicted by the model.

2 Establishing a surface chemical model for Cs^+ sorption onto bentonite

2.1 The composition of bentonite

For the evaluation of Cs^+ sorption onto bentonite, batch and diffusion measurements are carried out with Wyoming MX-80 bentonite and a mixture of 10:90 mass ratio of MX-80 bentonite and silica sand. The characterisation of the bentonite used in the experiments is given in Table 1. Calcite, gypsum and sodium chloride are the main reactive impurities. For modelling purposes we assume that the available sodium chloride is instantly dissolved. This assumption is also made for gypsum as long as it is below its saturation limit. Calcite dissolution is controlled by calcite equilibrium with the aqueous phase.

2.2 The compostion of the porewater

The knowledge of the porewater composition is of crucial importance for the modelling of ion exchange and surface complexation reactions at the bentonite surface, even for elements such as

Table 1 Data and composition of the Wyoming MX-80 bentonite.

Property		Value	Ref. [1]
Cation exchange capacity (CEC):	non-compacted bentonite	85 meq/100 g	1
	compacted bentonite	10 meq/100 g [2]	
Exchangeable cations (percentage distribution):			
	Na^+	81.7 %	2
	K^+	0.3 %	2
	Mg^{2+}	3.9 %	2
	Ca^{2+}	14.1 %	calc.[3]
Dry density, ρ_d, of compacted bentonite		2.00 g/cm^3	3
Density, ρ_w, of compacted, water saturated bentonite		2.30 g/cm^3	4
Porosity, ε, of compacted bentonite		0.30	4
Solid/porewater ratio in compacted bentonite		6.7 g/cm^3	calc.
$CaCO_3$ impurities in the bentonite		1.4 % (wt)	2
$CaSO_4$ impurities in bentonite		0.34 % (wt)	5
NaCl impurities in bentonite		0.007 % (wt)	5

[1] References: 1: Wieland et al. (1994), 2: Müller-Vonmoos and Kahr (1983), 3: Albinsson and Engkvist (1991), 4: derived and recalculated from Albinsson and Engkvist (1991), 5: Wanner et al. (1992).

[2] The value CEC = 10 meq/100 g is derived for compacted bentonite in this report.

[3] The value for Ca^{2+} reported could be subject to systematic error, cf. Wanner (1986). The value used here represents the complementary value to the CEC.

caesium that exhibit no significant interaction with the groundwater components. The chemical composition of the porewater in bentonite results from the interaction of groundwater with bentonite.

Model computations are performed with the surface chemical model developed by Wanner (1986), and refined by Wanner et al. (1992) and Wieland et al. (1994). The model accounts for ion exchange reactions, acid/base reactions at edge OH sites of montmorillonite and the presence of impurities ($CaCO_3$, $CaSO_4$, NaCl) in bentonite as given in Table 1.

In Table 2, the composition of Swedish groundwaters (Allard water and water from the Äspö site) are listed together with calculated porewater compositions for compacted Wyoming MX-80 bentonite in contact with Allard groundwater and with Äspö groundwater, respectively.

In the diffusion experiments performed by Albinsson and Engkvist (1991), the composition of the porewater in the bentonite/sand mixture (10/90) was not analysed. The water used for the experiments was Allard water, a low ionic strength granitic groundwater also known as the Standard Swedish Groundwater. The bentonite used was Wyoming MX-80 bentonite whose composition is given in Table 1. The chemical composition of porewater in a 10% bentonite and 90% sand mixture, predicted from model calculations for two different cation exchange capacities (CEC), is shown in Table 3.

Table 2 Composition of Allard groundwater and Äspö groundwater, as well as the predicted porewater of compacted Wyoming MX-80 bentonite in contact with Allard and Äspö groundwaters (GW) at 25°C. The concentration units are [mol dm^{-3}]. Note that the pH values are significantly lower than predicted with the earlier model of Wanner (1992) and Wanner et al. (1992). This is due to the consideration of the acid/base chemistry of the edge sites of montmorillonite, cf. Wieland et al. (1994).

	Allard groundwater (simplified)	MX-80 porewater (Allard GW)	Äspö groundwater (simplified)	MX-80 porewater (Äspö GW)
Na+	2.26E-3	1.62E-1	1.31E-1	3.36E-1
K^+	1.00E-4	1.58E-5	-	8.09E-6
Mg^{2+}	1.90E-4	2.40E-3	2.06E-3	6.00E-3
Ca^{2+}	4.64E-4	8.02E-3	1.10E-1	3.71E-2
Cl^-	1.48E-3	3.08E-3	3.40E-1	3.45E-1
SO_4^{2-}	1.00E-4	8.67E-2	7.40E-3	3.24E-2
SiO_2	1.39E-4	1.06E-4	-	1.07E-4
Alk	1.80E-3	3.62E-3	1.80E-4	3.05E-3
pH	8.12	7.36	7.38	6.78
Ionic strength	0.004	0.176	0.46	0.385

Table 3 Composition of the porewater calculated with the bentonite model for a compacted mixture of 10% Wyoming MX-80 bentonite and 90% silica sand, at 25°C. Units are [mol dm^{-3}].

Parameter	Porewater in a 10/90 bentonite/sand mixture, CEC in meq/100 g.	
	CEC = 85 [1])	CEC = 10 [1])
Na^+	4.30E-2	2.90E-2
K^+	4.81E-4	3.10E-4
Mg^{2+}	1.05E-4	2.20E-4
Ca^{2+}	4.57E-4	2.91E-3
Cl^-	1.26E-3	1.40E-3
SO_4^{2-}	1.16E-2	1.16E-2
SiO_2	1.53E-4	1.53E-4
Alk	6.06E-2	5.13E-3
pH	7.79	7.22
Ionic strength	4.86E-2	4.19E-2

[1]) CEC = 85 meq/100 g (cf. Table 1) was determined using a batch method. We find that the effective CEC in compacted bentonite is lower by a factor of about 8, i.e., CEC = 10 meq/100 g, cf. Section 3.3. The effective CEC of compacted bentonite is empirically derived from batch vs. diffusion experiments and indicates the loss of available ion exchange sites by compacting the bentonite, cf. Wieland et al. (1994).

2.3 *A surface chemical model for Cs^+ sorption onto Wyoming MX-80 bentonite*

2.3.1 *Experimental method*

The K_d values for Cs^+ sorption are experimentally determined in batch-type experiments conducted in polycarbonate tubes (15 ml). A weighted amount of untreated Wyoming MX-80 bentonite (0.1 or 1 g dm^{-3}) is equilibrated with 10 ml of a solution containing 0.2 ml ^{137}Cs stock solution and a known concentration of the background electrolyte (NaCl, $NaNO_3$, KCl, $CaCl_2$, $CaNO_3$, $MgCl_2$). In some experiments, Allard (low saline) and Äspö (high saline) groundwaters are used as background electrolyte. The activity of the ^{137}Cs stock solution is 2×10^6 cpm/ml. The total concentration of ^{137}Cs used in the experiments ranges from 10^{-8} to 10^{-9} M. After an equilibration time of 3 and 8 days, aliquots of the supernatant were analysed for ^{137}Cs using NaI(Tl)-detector (Intertechnique CG-4000). Each K_d value is calculated as average value from three individual samples.

2.3.2 *Modelling approach*

Table 4 summarises the ion exchange reactions and protolysis reactions considered for modelling Cs^+ sorption onto montmorillonite. The dissolution of impurities, the calcite equilibrium and the acid/base properties of edge OH sites control the chemical composition of the supernatant in diluted bentonite suspensions as well as the porewater of highly compacted bentonite. Na^+, K^+, Ca^{2+} and Mg^{2+} compete with Cs^+ for sorption onto surface sites (i.e., layer sites). Ion exchange reactions with two types of layer sites, denoted as X and Y sites, are considered in the proposed bentonite model (Wieland et al., 1994). A model with two layer sites, X and Y, accounts for differences in the affinity of the layer sites for protons. It is postulated that the X and Y sites represent the structural-charge sites of the external and internal surface, respectively. The differentiation in two types of layer sites is especially relevant when ion exchange reactions in near-neutral solutions of low ionic strength are modelled. The surface

Table 4 Reactions and parameters of the surface chemical model for bentonite.

	logK°	Reference
Reactions:		
$\equiv SOH_2^+ \Leftrightarrow \equiv SOH + H^+$	−5.4	Wieland et al. (1994)
$\equiv SOH \Leftrightarrow \equiv SO^- + H^+$	−6.7	Wieland et al. (1994)
$H^+ + NaX \Leftrightarrow HX + Na^+$	4.57	Wieland et al. (1994)
$K^+ + NaX \Leftrightarrow KX + Na^+$	0.26	Fletcher and Sposito, 1989
$Cs^+ + NaX \Leftrightarrow CsX + Na^+$	1.60	this study
$Ca^{2+} + 2\,NaX \Leftrightarrow CaX_2 + 2\,Na^+$	0.21	Wanner et al. (1992)
$Mg^{2+} + 2\,NaX \Leftrightarrow MgX_2 + 2\,Na^+$	0.13	Wanner et al. (1992)
$H^+ + NaY \Leftrightarrow HY + Na^+$	3.00	Wieland et al. (1994)
$K^+ + NaY \Leftrightarrow KY + Na^+$	0.26	Fletcher and Sposito, 1989
$Cs^+ + NaY \Leftrightarrow CsY + Na^+$	1.60	this study
$Ca^{2+} + 2\,NaY \Leftrightarrow CaY_2 + 2\,Na^+$	0.21	Wanner et al. (1992)
$Mg^{2+} + 2\,NaY \Leftrightarrow MgY_2 + 2\,Na^+$	0.13	Wanner et al. (1992)
Parameters:		
Site density of edge OH sites [mol/g]	2.8×10^{-5}	
Site density of X layer sites [meq/100 g]	1.70	
site density of Y layer sites [meq/100 g]	83.30	

chemical ion pair formation constant of Na^+ is fixed at $\log K^\circ = 20$, in such a way that no unoccupied (i.e., charged) layer sites exist (Wanner, 1986). The exchange constant for K^+ given in Table 4 is from Fletcher and Sposito (1989). Table 4 shows that the exchange constant for H^+ is different for X and Y layer sites. Apparently, X layer sites reveal a higher affinity for protons than Y layer sites. The constant for Cs^+ is treated as a fit parameter. Furthermore it is assumed that the exchange constant for Cs^+ is the same for X and Y layer sites. The exchange constant for Cs^+ is derived from the batch-type experiments presented in the following section. A ^{137}Cs concentration of 10^{-9} M is assumed for the model computations.

2.3.3 Modelling batch type experiments with Wyoming MX-80 bentonite

The distribution coefficient, K_d, describes the ratio of the concentrations of sorbed and dissolved species of a radionuclide:

$$K_d = \frac{[Cs]_{sorbed} \quad [mol/kg]}{[Cs]_{dissolved} \quad [mol/m^3]} \tag{1}$$

Figure 1 shows batch type sorption experiment conducted with Wyoming MX-80 bentonite in solutions of various compositions and solid/water ratios. The data set covers experiments done over a large range of ionic strengths. The values are listed in Table 5. Experiments are conducted with NaCl, $NaNO_3$, KCl, $CaCl_2$, $CaNO_3$ and $MgCl_2$ solutions, as well as with Allard and Äspö groundwaters. The ion exchange constant for Cs^+ sorption is determined in such a manner to achieve best agreement between the K_d value for Cs^+ predicted from model computations and the experimental K_d values. The use of an exchange constant for the Cs^+/Na^+ exchange of $\log K_{ex}^\circ = 1.6$ results in a good agreement between the calculated and experimental K_d values, cf. Figure 1. Significant deviations between predicted and experimental values are observed for low bentonite-to-water ratios in $CaCl_2$ and $MgCl_2$ solutions. The discrepancies may be due to experimental limitations and/or limitations in model computations, but also to the fact that the relative importance of the experimental errors increases at low suspension concentrations. Ion exchange reactions at the montmorillonite/water interface are simulated as hypothetical surface complexation reactions according to Fletcher and Sposito (1989). In the concept of Fletcher and Sposito (1989) the equilibrium constants for heterovalent ion exchange reactions, e.g., Ca^{2+} and Mg^{2+} for Na^+ on montmorillonite, depend on the level of exchange, i.e., the mole fraction of the exchangeable cations on the surface. It is possible that this dependence overrates the affinity of Ca^{2+} and Mg^{2+} to the surface sites and thus their competition with Cs^+ under certain conditions. This may explain the discrepancy between experimental and calculated K_d values at low bentonite/water ratios.

Model computations are also performed by considering the stability of calcium and magnesium chloride ion pairs in aqueous solution (Johnson and Pytkowicz, 1979; Williams-Jones and Seward, 1989) and the formation of surface complexes of $CaCl^+$ and $MgCl^+$ with surface layer sites. However, agreement between predicted and experimental K_d values cannot be improved

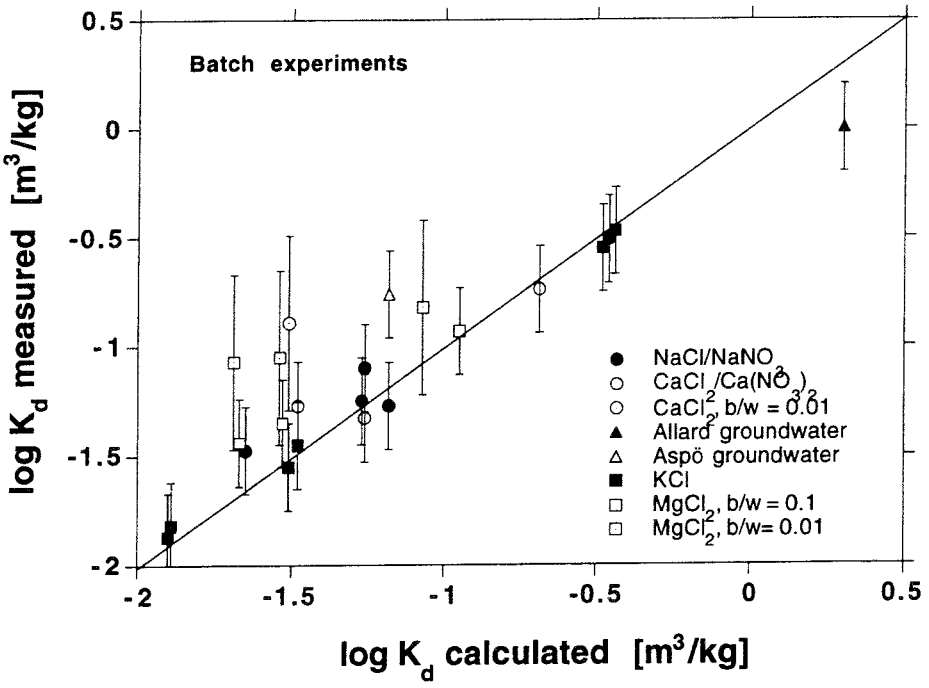

Figure 1 *Comparison of measured and calculated logK_d values for Cs^+ sorption in bentonite. Uncertainties in logK_d are estimated to ±0.2. Uncertainties in logK_d for the experiments conducted at low bentonite/solution ratios are estimated to ±0.4. The experimental conditions are as follows: The bentonite/water (b/w) ratio is 0.1 g/ml and 0.01 g/ml except for experiments conducted in Äspö groundwater (0.18 g/ml). The concentrations of the electrolyte background are 1 M, 0.5 M and 0.05 M for NaCl, KCl and $MgCl_2$, and 0.25 M and 0.025 M for $CaCl_2$. In two of the experiments 0.5 M $NaNO_3$ and 0.25 M $Ca(NO_3)_2$ are used as background electrolyte. The compositions of Allard and Äspö groundwater are given in Table 2.*

when ion pair formation and surface complex formation of $CaCl^+$ and $MgCl^+$ are considered. Association of calcium and magnesium ions with chloride in aqueous solution at low temperature is dominated by weak, outer sphere complexes. The stability constants of the ion pair formations of calcium and magnesium chloride in solution are thus small and, furthermore, ill-defined. There are still controversial views in the literature regarding the importance of $CaCl^+$ and $MgCl^+$ surface complexes. Since unambiguous information is not available concerning both ion pair formation in solution and surface complex formation of $CaCl^+$ and $MgCl^+$, we do not consider the corresponding thermodynamic equilibrium reactions in the model presented in this report.

Table 5 Compilation of batch K_d values for Cs^+ in pure Wyoming MX-80 bentonite and mixtures of 10% bentonite and 90% quartz sand.

b/w [1] [g/cm^3]	s/w [2] [g/cm^3]	Water type	K_d(meas) [m^3/kg]	pH [3]	K_d(ix) [4] [m^3/kg]	K_d(ix) [5] [m^3/kg]
Pure bentonite:						
0.102	0.102	1 M NaCl	0.034	7.38	0.022	
0.104	0.104	0.5 M NaCl	0.056	7.41	0.054	
0.104	0.104	0.5 M $NaNO_3$	0.054	7.55	0.066	
0.011	0.011	0.5 M NaCl	0.080	8.81	0.055	
0.104	0.104	0.05 M NaCl	0.310	8.12	0.344	
0.104	0.104	0.25 M $CaCl_2$	0.053	6.61	0.033	
0.103	0.103	0.25 M $Ca(NO_3)_2$	0.047	6.61	0.052	
0.103	0.103	0.025 M $CaCl_2$	0.183	7.39	0.205	
0.010	0.010	0.25 M $CaCl_2$	0.148	7.15	0.031	
0.1	0.1	1 M KCl	0.015	8.07	0.013	
0.1	0.1	0.5 M KCl	0.036	8.03	0.033	
0.1	0.1	0.05 M KCl	0.342	8.66	0.364	
0.01	0.01	1 M KCl	0.015	9.43	0.013	
0.01	0.01	0.5 M KCl	0.028	9.34	0.031	
0.01	0.01	0.05 M KCl	0.280	9.33	0.329	
0.1	0.1	1 M $MgCl_2$	0.036	6.96	0.021	
0.1	0.1	0.5 M $MgCl_2$	0.045	7.05	0.030	
0.1	0.1	0.05 M $MgCl_2$	0.117	7.72	0.113	
0.01	0.01	1 M $MgCl_2$	0.084	7.54	0.021	
0.01	0.01	0.5 M $MgCl_2$	0.089	7.62	0.029	
0.01	0.01	0.05 M $MgCl_2$	0.150	8.09	0.085	
0.01	0.01	Allard water	1.0	9.53	2.03	
0.18	0.18	Äspö water	0.172	7.16	0.076	
10% bentonite and 90% quartz sand:						
0.01	0.1	1 M KCl	0.001	9.30	0.001	0.005
0.01	0.1	0.5 M KCl	0.003	9.10	0.003	0.010
0.01	0.1	0.05 M KCl	0.020	9.30	0.033	0.129
0.01	0.1	1 M $MgCl_2$	0.015	7.00	0.0003	0.001
0.01	0.1	0.5 M $MgCl_2$	0.018	7.31	0.0014	0.005
0.01	0.1	0.05 M $MgCl_2$	0.025	8.01	0.008	0.032
0.0011	0.010	0.25 M $CaCl_2$	0.093	7.90	0.003	0.011
0.0012	0.010	0.5 M NaCl	0.033	9.13	0.006	0.022
0.018	0.20	Äspö water	0.030	7.45	0.008	0.025

[1] b/w denotes the bentonite-to-water ratio [g/cm^3].
[2] s/w denotes the solid-to-water ratio [g/cm^3] .
[3] pH is calculated from model computation.
[4] K_d(ix) is modelled with $\log K_{ex}^\circ = 1.6$ as the exchange constant for Cs^+/Na^+.
[5] For comparison, K_d(ix) is modelled with $\log K_{ex}^\circ = 2.2$ as the exchange constant for Cs^+/Na^+.

2.3.4 *Modelling batch type experiments of bentonite/sand mixtures*

Measured and calculated distribution coefficients, K_d, determined in mixtures of 10% Wyoming bentonite MX-80 and 90% quartz sand (by weight) are compared in Figure 2 and also listed in Table 5. Experiments are conducted for low benonite/water ratios (e.g., b/w < 0.02 g/cm^3) in NaCl, KCl, $CaCl_2$, and $MgCl_2$ solutions as well as in Äspö groundwater. The model computations are done with a Cs^+/Na^+ exchange constant of $\log K_{ex}^\circ = 1.6$. Figure 2 reveals a large scattering of the predicted and measured K_d values. Agreement between modelled and experimental values can be slightly improved by increasing the exchange constant to $\log K_{ex}^\circ = 2.2$, possibly due to adsorption of Cs^+ onto quartz sand. Silanol sites are exposed at the surface of quartz sand and may act as coordinative functionalities for Cs^+. However, for the bentonite/sand mixtures with NaCl and KCl as background electrolyte, modelling computations with $\log K_{ex}^\circ = 2.2$ significantly overestimate adsorption of Cs^+. A lack of experimental data for Cs^+ sorption onto quartz precludes, at present, a detailed mechanistic modelling of Cs^+ sorption in a bentonite/quartz mixture. An explanation for the discrepancy between predicted and experimental K_d values and their dependence of the type of electrolyte background cannot be given at present. The discrepancy may again be due to experimental or modelling errors as mentioned in the previous section.

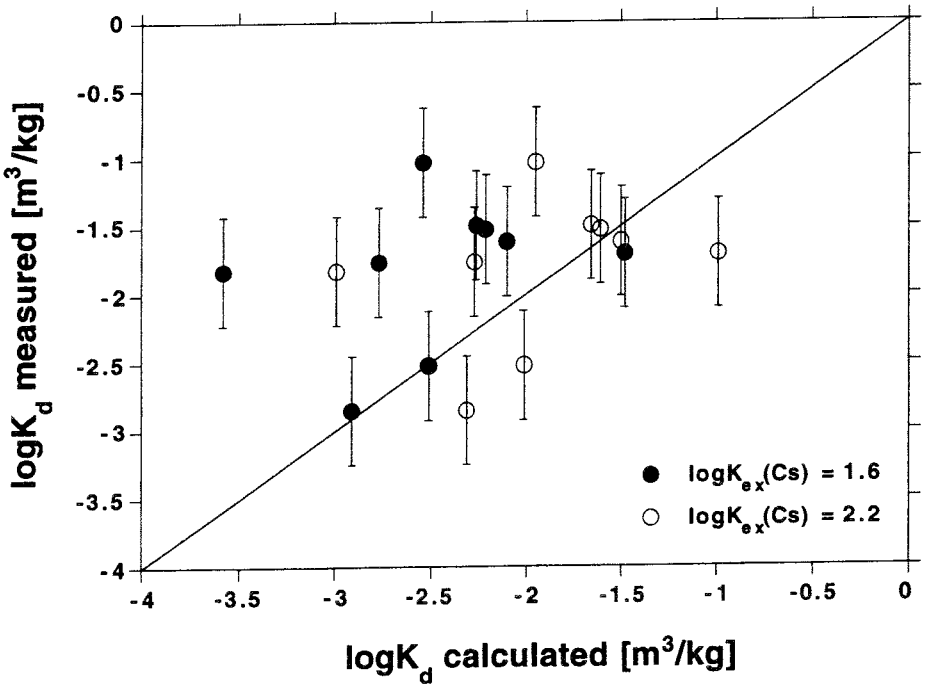

Figure 2 *Comparison of measured and calculated $\log K_d$ values for Cs^+ sorption in 10/90 bentonite/sand mixtures. Uncertainties are estimated to ±0.4 in $\log K_d$. The bentonite-to-water ratios (b/w) are 0.001 g/ml, 0.01 g/ml and 0.018 g/ml (Äspö groundwater), respectively. The concentrations of the electrolyte background are 1 M, 0.5 M and 0.05 M for KCl and $MgCl_2$ solutions, 0.5 M for NaCl and 0.25 M for $CaCl_2$ electrolytes.*

2.3.5 *Modelling batch type experiments as a function of Cs^+ concentration*

The distribution coefficients, K_d, are also measured as a function of the ^{134}Cs concentration ranging from 10^{-9} M to 10^{-1} M. Calculated and measured K_d values are displayed in Figure 3 and listed in Table 6. Agreement between predicted and measured data is good if we take into account the uncertainties in the experimental data. Table 6 shows that the predicted and experimental K_d values agree well at low and very high Cs^+ concentrations. The difference between modelled and experimental distribution coefficients increases with increasing Cs^+ concentration and reaches a maximum at 3×10^{-4} M Cs^+. However, the difference is less than a factor of about 2. In the presented bentonite model, two types (X and Y) of layer sites with the same affinity for Cs^+ are considered with $\log K_{ex}^{\circ} = 1.6$ for both surface sites. Therefore the proposed model actually corresponds to a simple one-site model with respect to Cs^+ sorption. The observed discrepancy between the predicted and experimental K_d values is most likely due to the presence of more than one type of layer surface sites for Cs^+ sorption. A multi-site model would require different exchange constants for Cs^+ for different types of layer sites.

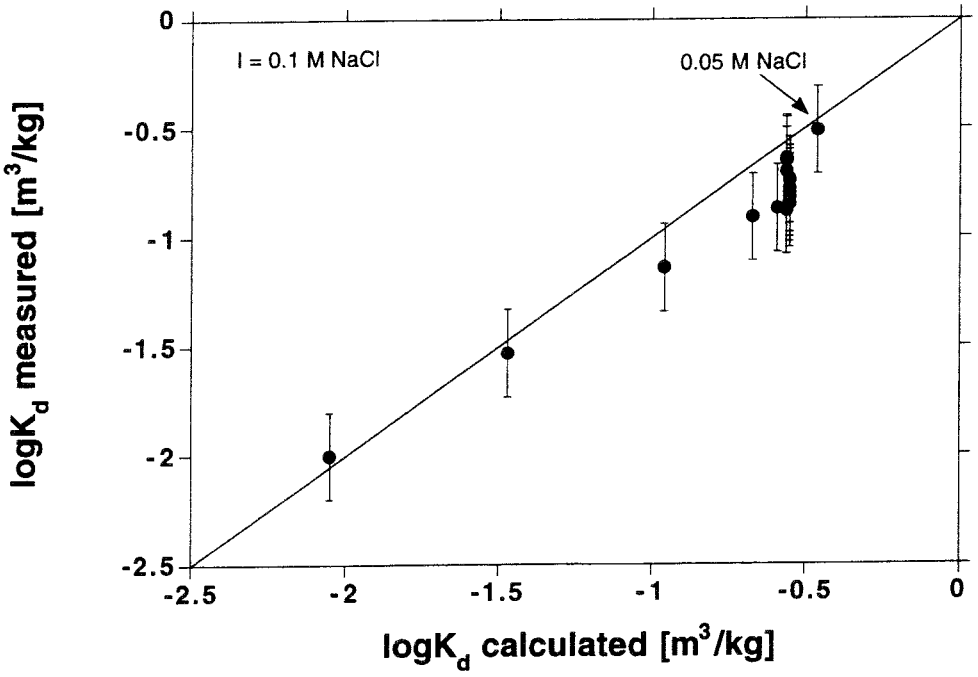

Figure 3 *Comparison of measured and calculated $\log K_d$ values for Cs^+ sorption for ^{134}Cs concentrations ranging from 10^{-9} M to 10^{-1} M. Uncertainties are estimated to ±0.2 in $\log K_d$. The experimental conditions are: bentonite/water ratio = 0.01 g/ml, I = 0.1 M (NaCl) unless otherwise stated.*

Table 6 Batch K_d values for pure Wyoming MX-80 bentonite as a function of ^{134}Cs concentration (bentonite/water = 0.01 g/cm^3, background electrolyte: 0.1 M NaCl).

Cs concentration [M]	K_d (meas) [m^3/kg]	pH [1]	K_d (ix) [m^3/kg]
1E-1	0.010	9.13	0.009
3E-2	0.030	9.11	0.034
1E-2	0.072	9.12	0.110
3E-3	0.124	9.14	0.214
1E-3	0.133	9.16	0.259
3E-4	0.133	9.18	0.273
1E-4	0.140	9.18	0.281
3E-5	0.152	9.18	0.282
1E-5	0.158	9.18	0.283
3E-6	0.167	9.18	0.281
1E-6	0.188	9.18	0.284
3E-7	0.200	9.18	0.285
1E-7	0.222	9.18	0.284
3E-8	0.224	9.18	0.286
1E-8	0.231	9.18	0.288
1E-9 [2]	0.309		0.347

[1] pH is calculated from model computations.
[2] The background electrolyte is 0.05 M NaCl here, rather than 0.1 M NaCl.

This experiment shows that the site saturation is predicted correctly by the model. It is seen from Table 6 that both the measured and predicted K_d values decrease significantly above a Cs concentration of about 3×10^{-3} M. This is explained by the CEC due to which 8.5×10^{-3} moles of surface sites are available per litre of water at the present bentonite/water ratio of 0.01 g/cm^3. It should be noted, however, that bentonite may contain up to 0.8 ppm Cs (Snellman et al., 1987) which corresponds to 6×10^{-8} M Cs at the current solid/liquid ratio. It is thus probable that the lowest possible concentration of Cs under the present conditions is 6×10^{-8} M and that the three or four lowest concentrations in Table 6 are not correct. However, since the theoretical model is a one-site model predicting concentration-independent sorption in the undersaturated region, this error does not influence the results of the comparison. Under these considerations, the presented one-site surface chemical model for Cs^+ sorption onto bentonite allows to predict K_d values within a factor of 2 for Cs^+ concentrations ranging from $\leq10^{-7}$ M to 10^{-1} M.

3 Interpreting and modelling Cs^+ sorption in diffusion experiments

The proposed surface chemical model is further applied to predicting the distribution coefficient of Cs^+ onto montmorillonite in compacted bentonite. The experimental K_d values result from diffusion experiments conducted by Albinsson and Engkvist (1991).

3.1 Derivation of Cs^+ concentration levels in the diffusion experiments

The analysed concentrations of ^{134}Cs on the solid in the diffusion experiment of Albinsson and Engkvist (1991) decrease from 36'000 to 55 cpm/g between 0 and 18 mm migration path. The ^{134}Cs stock solution from Amersham contained about 0.44 g ^{134}Cs per litre and an activity of 2.25 Ci/L. The relationships between the concentration of Cs and the radiation characteristics of the stock solution are thus as follows:

$$1\ \text{Ci} = 0.20\ \text{mg}\ ^{134}\text{Cs}$$

or

$$1\ \text{Bq} = 3.9 \times 10^{-14}\ \text{mol}\ ^{134}\text{Cs}.$$

By assuming a detection efficiency of 40%, we have

$$1\ \text{Bq} = 9.8 \times 10^{-14}\ \text{mol}\ ^{134}\text{Cs}$$

or

$$1\ \text{cpm} = 1.6 \times 10^{-15}\ \text{mol}\ ^{134}\text{Cs}.$$

Hence, the maximum value of C_{max} = 36'000 cpm/g corresponds to $C_{max} = 6\times10^{-11}$mol/g added Cs, and the minimum value of C_{min} = 55 cpm/g corresponds to $C_{min} = 9\times10^{-14}$mol/g added Cs. These values represent the sum of the amounts of caesium sorbed and in solution.

Since we use a solution model, we need to know the total amount of Cs^+ present per litre of aqueous phase, both sorbed and dissolved. Thus, we multiply the solid concentration values derived above by the value of the solid/porewater ratio (6.7 g/cm^3) from Table 1. The total maximum and minimum concentrations and the amounts sorbed and dissolved, expressed in moles per litre of porewater, are thus:

$$[Cs]_{t,max} = 4 \times 10^{-7}\ \text{mol/L}$$

$$[Cs]_{t,min} = 6 \times 10^{-10}\ \text{mol/L}.$$

The clay was pre-equilibrated with the appropriate water before it was mixed with the silica sand. The mixture was then compacted to a density of 2 g/cm^3 and submerged with the aqueous phase. The composition of the solid phase used in the experiments is given in Table 1. For the evaluations, it is assumed that the proportion of the nuclide sorbing on the surface of the silica sand is negligible with respect to that sorbing on the bentonite. The solid is thus considered as a "dilute bentonite".

3.2 *Estimating the pore diffusivity, D_p, for compacted Wyoming MX-80 bentonite*

The key parameter that results from diffusion experiments is the apparent diffusivity, D_a, of a nuclide. The relationship between D_a and the distribution coefficient, K_d, is

$$\frac{D_p}{D_a} = 1 + \left(\frac{\rho_d}{\varepsilon}\right)K_d \qquad (2)$$

where ε is the porosity by volume, ρ_d the dry density of the solid and D_p the pore diffusivity without sorption. Some authors prefer to use the specific density, ρ_s, and they replace ρ_d in Eq.(2) by $\rho_s(1-\varepsilon)$. D_a is an experimentally observed parameter; it represents the main result of a diffusion measurement. The quality of the derived K_d depends on the quality of the estimation of D_p or of the experimental determination of D_p by the use of the stationary diffusion technique if possible, cf., e.g., Neretnieks (1985). The porosity, ε, represents the pore space available for diffusion. Hence, in compacted bentonite the value of ε will be significantly lower than the bulk porosity calculated by use of the equation

$$\varepsilon = 1 - \frac{\rho_d}{\rho_s} \qquad (3)$$

However, due to the lack of information and as a preliminary assumption, the diffusion porosity used in Eq. (2) is approximated by the bulk porosity and calculated by Eq. (3). The knowledge of the pore diffusivity is of crucial importance for the determination of K_d values and the evaluation of surface reaction mechanisms. The quality of the derived K_d depends on the quality of the estimation of D_p. It is possible that part of the scatter of K_d reported in the literature from diffusion experiments is due to the use of inconsistent values for D_p. A more detailed discussion of the problems in deriving consistent data sets of D_p, ε and K_d is presented in the Appendix "Diffusivities and K_d's" of the present report.

We assume that the diffusivity of tritiated water, HTO, measured in Kunigel-V1 by Sato et al. (1993) at different dry density values is an adequate approximation of the pore diffusivity, D_p, in Wyoming MX-80 bentonite. We also assume that the dependence of D_p on the dry density of bentonite observed in Kunigel-V1 also applies to Wyoming MX-80 bentonite. In the following, we would like to justify the proposed assumption.

In Section 2.2 we show that the chemical composition of porewater is controlled by the reactions of the montmorillonite surface with dissolved species and by the dissolution of impurities, i.e., calcite, sodium chloride and calcium sulfate, in bentonite. Table 7 shows that the contents of Na-montmorillonite, calcite and the trace impurities are comparable in the two bentonites of different origin. The chemical compositions of the porewaters for Wyoming MX-80 and Kunigel-V1 bentonite are listed in Table 2 and Table 8, respectively. In the diffusion experiments of Albinsson and Engkvist (1991), compacted Wyoming MX-80 bentonite was in contact with Allard groundwater (Table 2). Sato et al. (1993) used distilled water as a transport media. Our calculations, however, show that irrespective of the initial composition of the water

Table 7 The composition of Wyoming MX-80 (Müller-Vonmoos and Kahr, 1983) and Kunigel-V1 (Sato et al., 1993) bentonite.

		Wyoming MX-80	Kunigel-V1
Minerals:			
	Na-montmorillonite	75	50 - 55
	Quartz	15	30 - 35
	Feldspar	5 - 8	5 - 10
	Zeolite	-	1 - 2
	Calcite	1.4	1 - 3
	Dolomite	-	1 - 2
	Pyrite	0.3	0.3 - 0.6
Trace impurities:			
	KCl + NaCl	0.007 [1)]	0.0055 [2)]
	$CaSO_4$	0.34 [1)]	0.38 [2)]

[1)] cf. Table 1.
[2)] cf. Wanner and Wieland (1993).

Table 8 The chemical composition of the porewater of compacted Kunigel-V1.

Parameter	Kunigel-V1 (CEC = 85 meq/100 g)
Na^+	1.74 E-1 mol dm^{-3}
K^+	8.54 E-5 mol dm^{-3}
Mg^{2+}	2.39 E-3 mol dm^{-3}
Ca^{2+}	8.17 E-3 mol dm^{-3}
Cl^-	9.35 E-3 mol dm^{-3}
SO_4^{2-}	8.85 E-2 mol dm^{-3}
SiO_2	1.07 E-4 mol dm^{-3}
alkalinity	3.22 E-3 mol dm^{-3}
pH	7.41
ionic strength	9.90 E-2 mol dm^{-3}

used in the diffusion experiments, the porewater composition of compacted Kunigel-V1 (Table 8) and compacted Wyoming MX-80 (Table 2) bentonite are almost identical, i.e., the concentrations of major cations Na^+, Mg^{2+} and Ca^{2+} as well as pH are similar.

Caesium sorption onto montmorillonite in compacted bentonite strongly depends on the chemical composition of the porewater. We therefore expect comparable values of apparent diffusivities of corresponding cations and anions in compacted Kunigel-V1 and compacted Wyoming MX-80 bentonite. In Figure 4, the apparent diffusivities of ^3H, ^{99}Tc, ^{137}Cs, ^{237}Np and ^{241}Am in compacted Kunigel-V1 bentonite (Sato et al., 1993) and compacted Wyoming MX-80 bentonite (Albinsson and Engkvist, 1991; Torstenfelt and Allard, 1986) are compared. The two data sets of apparent diffusivities for ^{99}Tc, ^{137}Cs, ^{237}Np and ^{241}Am measured in Kunigel-V1 and Wyoming MX-80 bentonite are consistent. We hence may infer that the apparent diffusivity of tritiated water, HTO, represents the reference diffusivity in both compacted Kunigel-V1 and compacted Wyoming MX-80 bentonite. It therefore seems appropriate to use the apparent diffusivity of ^3H as the reference diffusivity for Cs^+ for compacted Wyoming MX-80 bentonite and 10/90 bentonite/sand mixtures of Wyoming MX-80.

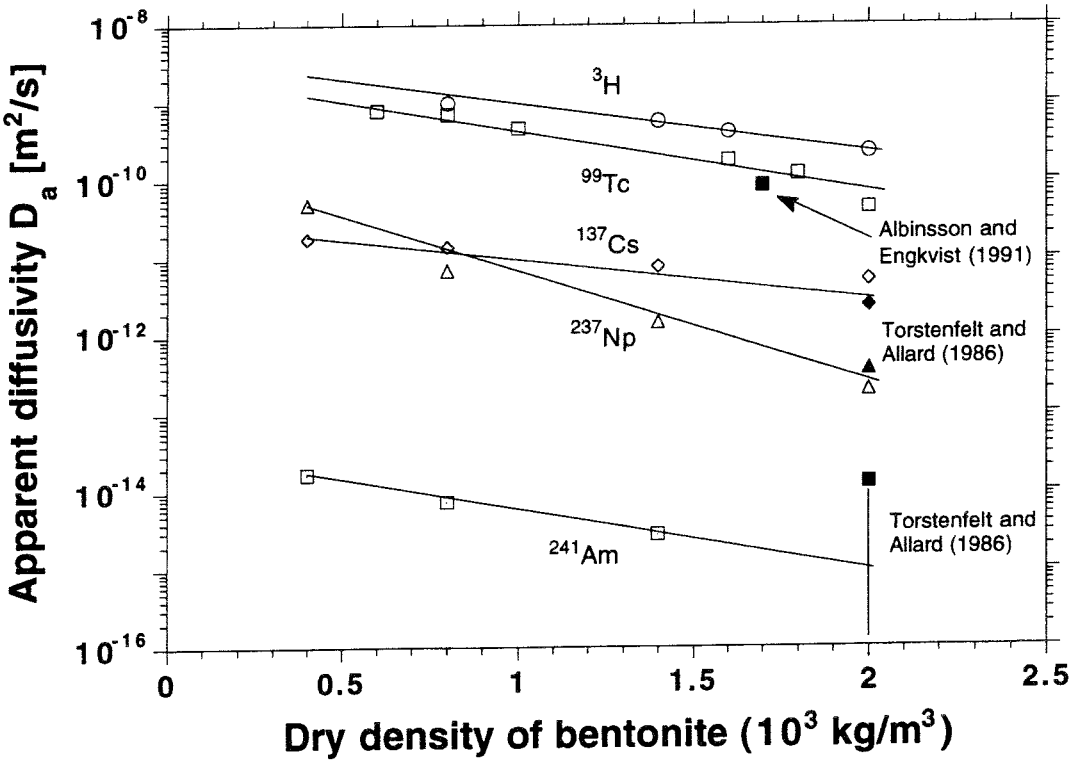

Figure 4 *Apparent diffusivities of ^3H, ^{99}Tc, ^{137}Cs, ^{237}Np and ^{241}Am as a function of the dry density in Kunigel-V1 (Sato et al., 1993) and Wyoming MX-80 bentonite (Albinsson and Engkvist, 1991; Torstenfelt and Allard, 1986). The apparent diffusivity, D_a, of HTO is used as pore diffusivity of caesium.*

3.3 *Derivation of the modelling parameters in compacted bentonite*

Based on the analysis of the results obtained from batch type experiments, we recommend to use the caesium exchange constant of $\log K_{ex}^{\circ} = 1.6$ evaluated in Section 2.3 for modelling Cs^+ sorption in compacted bentonite. This constant is evaluated from batch type experiments conducted in suspensions with bentonite/water ratios ranging from 0.001 to 0.1 g/ml. However, the compaction of bentonite to a dry density of 2000 kg/m^3 may cause a loss of available ion exchange sites. For the estimation of the relevant CEC of compacted bentonite, the experimental K_d values determined in the diffusion experiments conducted with Wyoming MX-80 bentonite and Allard groundwater are compared with values obtained from the model computations. The predicted K_d values are based on the Cs^+/Na^+ exchange constant of $\log K_{ex}^{\circ} = 1.6$ and depend on the CEC used in the bentonite model. For CEC = 85 meq/100g, the K_d value is estimated to $K_d = 0.124$ which is too high compared to the experimental values under these conditions, cf. Table 9 (References 1, 3, 6 and 8, cf Footnote 5). Agreement between experimental and predicted K_d values is achieved if the CEC of compacted bentonite is reduced to 10 meq/100g ($K_d = 0.024$). Therefore we use

$$\text{CEC of compacted bentonite } (\rho_d = 2000 \text{ kg/m}^3) = 10 \text{ meq/100g}$$

for modelling Cs^+ sorption in compacted bentonite. This value is needed to obtain consistency within the model. However, the fact that the model is internally consistent does not imply that it is also externally consistent, i.e., the CEC value derived above cannot be considered to be a measure for the reduction of available pore space in compacted bentonite. This is because the errors made in estimating the pore diffusivity of Cs^+ and by using Eq. (3) to calculate the diffusion porosity (cf. Section 3.2) are implicitely contained in the value of 10 meq/100g derived for the CEC in compacted bentonite. It is recommended to work in the direction of establishing both internally and externally consistent (i.e., realistic) sets of D_p, ε and K_d. A more detailed discussion of this problem is given in the Appendix.

3.4 *Derivation of the distribution coefficient for Cs^+ from diffusion experiments*

Table 9 shows a compilation of published diffusivities of Cs^+ in Kunigel-V1 and Wyoming MX-80 bentonite. Most experiments were conducted with Allard water. The pore diffusivities of Cs^+, D_p, listed in Table 9 correspond to the diffusivities of HTO at the respective dry densities of bentonite. The experimental K_d values are determined according to Eq. (2). The porosities of bentonite are calculated with Eq. (3) using $\rho_s = 2.7 \times 10^3$ kg/m^3. For the dry densities of 1750 kg/m^3 and 2105 kg/m^3, the calculated values of ε are 0.35 and 0.22, respectively, which compare well with the measured values of 0.35 and 0.25, respectively.

Experimental and calculated K_d values are listed in Table 9 and displayed in Figure 5. The calculated K_d values are denoted as K_d(ix) in the Table 9. The agreement is fair for most distribution coefficients derived from diffusion experiments.

Table 9 Compilation of apparent diffusivities for Cs^+ and derived K_d values in Wyoming bentonite MX-80 and Kunigel-V1 bentonite from different sources.

Solid phase	ρ_d [kg/m^3]	Water type	D_a [m^2/s]	K_d(rep)[1] [m^3/kg]	D_p [2] [m^2/s]	K_d [3] [m^3/kg]	K_d(ix) [4] [m^3/kg]	Ref. [5]
MX-80	2000	Allard water	1.4 to 2E-12	0.13 to 0.19	2.5E-10	0.019 to 0.027	0.024	1
MX-80	1600 to 1800	Allard water	1 to 8E-12 [6]		3.2E-10 to 4.1E-10	0.006 to 0.071	0.028	2
MX-80	2000	Allard water	2.4E-12		2.5E-10	0.015	0.024	3
MX-80	2030	1.2M NaCl	6.5E-13	0.05	2.4E-10	0.055	0.004	4
	1980	0.6M NaCl	6.9E-13	0.09	2.6E-10	0.056	0.007	
	1870	0.2M NaCl	8.5E-13	0.21	2.9E-10	0.055	0.015	
	1910	0.02M NaCl	3.5E-13	0.85	2.8E-10	0.125	0.025	
	1940	0.003M NaCl	2.5E-13	1.80	2.7E-10	0.166	0.026	
MX-80	2105 [7]	Allard water	5E-13		2.2E-10	0.052	0.021	5
MX-80	2000	Allard water	3E-12		2.5E-10	0.012	0.024	6
Kunigel-V1	400	distilled water	1.8E-11		1.7E-9	0.204	0.574	7
	800		1.4E-11		1.1E-9	0.066	0.205	
	1400		7.8E-12		5.2E-10	0.024	0.073	
	2000		5.2E-12		2.5E-10	0.007	0.018	
MX-80	2000	Allard water	2.5E-12		2.5E-10	0.015	0.024	8
10/90 MX-80/ silica sand	2000	Allard water	5E-12		2.5E-10	0.007	0.005	9
MX-80	2000	Äspö water [8]	3.2E-12		2.5E-10	0.012	0.009	8
10/90 MX-80/ silica sand	2000	Äspö water [8]	6.5E-12		2.5E-10	0.006	0.0008	8

1) K_d values reported by the authors as derived from the diffusivities.
2) Pore diffusivity, D_p, of Cs^+ estimated by analogy with the diffusivity of HTO in Kunigel-V1 (Sato et al., 1993).
3) Calculated in this report from D_a and D_p.
4) K_d calculated by using the ion exchange model developed in this report.
5) 1: Torstenfelt et al. (1983), 2: Neretnieks (1985) (This is a compilation of earlier Swedish experiments), 3: Torstenfelt and Allard (1986), 4: Muurinen et al. (1986), 5: Albinsson et al. (1990), 6: Albinsson et al. (1993), 7: Sato et al. (1993), 8: Albinsson (1993), 9: Albinsson and Engkvist (1991).
6) Recommendation.
7) This is the correct dry density of the solid used in the experiments, as remeasured recently by Albinsson (1993a). The porosity is estimated to 0.25.
8) Water from the Äspö site at 860 m depth (KAS 03), ionic strength I=0.46 M, pH=8, high concentrations of NaCl and $CaCl_2$.

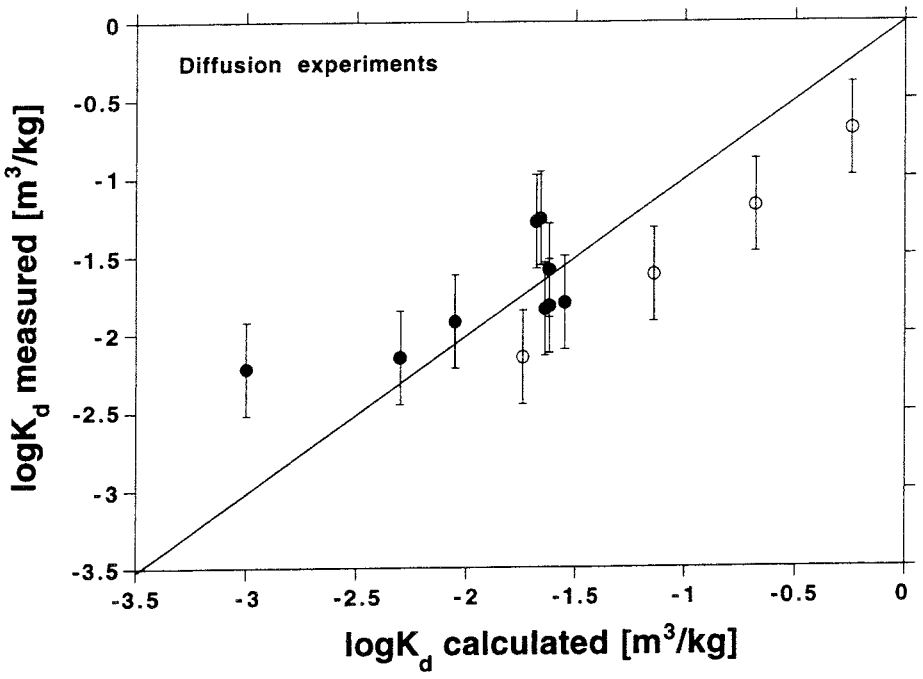

Figure 5 *Comparison of measured and calculated $logK_d$ values for Cs^+ in compacted Kunigel-V1 and Wyoming MX-80 bentonite as evaluated from diffusion experiments. Uncertainties are estimated to ±0.3 in $logK_d$. The experimental conditions and references are listed in Table 9. The data from Muurinen et al. (1986) are not included in the plot. Open circles represent the data from Sato et al. (1993).*

The simulation of the data in Refs. 1 (Torstenfelt et al., 1983) and 3 (Torstenfelt and Allard, 1986) are satisfactory. The K_d range resulting from the range of apparent diffusivities recommended by Neretnieks (1985) (Ref. 2 in Table 9) is simulated by using an average density of $\rho_d = 1700$ kg/m^3.

The experiments of Muurinen et al. (1986) (Ref. 4 in Table 9) were performed in NaCl solutions of different concentrations. The bentonite model underestimates Cs^+ sorption by a factor of 7 to 15. Possible sources for the discrepancy are difficult to envisage. It is, however, evident that the diffusivities measured by Muurinen et al. (1986) are very low compared to other measurements done under similar conditions. For example, the measurements conducted in 0.003 M NaCl by Muurinen et al. (1986) can be compared with the diffusion measurements in Allard groundwater reported by Torstenfelt and Allard (1986), and Albinsson et al. (1993). The experimental diffusivities are 2.5×10^{-13} and $2.4\text{-}3.0\times10^{-12}$ m^2/s ($\rho_d = 2000$ kg/m^3), respectively. The discrepancy is a factor of 10 and, hence, is of the same order of magnitude as the discrepancy between Muurinen's measurements and our model predictions.

A recent paper of Albinsson et al. (1990) reports apparent diffusivities on a number of nuclides in compacted bentonite of $\rho_d = 2000$ kg/m^3 reportedly. The low resulting values of the apparent

diffusivities induced the authors to redetermine the dry density of the solid used in those experiments. The resulting, correct dry density of the solid used by Albinsson et al. (1990) is $\rho_d = 2105$ kg/m^3 (Albinsson, 1993a) which is the value used in the model computations.

Albinsson et al. (1993) performed diffusion measurements from a spiked concrete phase (Standard Portland paste) into MX-80 bentonite pre-equilibrated with Allard water. They measured an apparent diffusivity for caesium of 3×10^{-12} m^2/s. With the pore diffusivity proposed in this report for compacted bentonite, $D_p = 2.5\times10^{-10}$ m^2/s, a K_d of 0.012 m^3/kg is calculated. The experimental value and the K_d calculated with the ion exchange model for pure bentonite ($K_d = 0.024$ m^3/kg) agree within the estimated uncertainties. This may indicate that the concrete phase exerts only a minor influence on the chemical composition of the porewater in compacted bentonite. A significant increase in the concentration of Ca^{2+} in the bentonite pore water would lead to a more important decrease in Cs^+ sorption.

Sato et al. (1993) carried out diffusion measurements using Kunigel-V1 and distilled water. Kunigel-V1 contains about 55% Na-montmorillonite. The CEC of dispersed Kunigel-V1 bentonite is not reported by Sato et al. (1993) and is estimated here to 60 meq/100g based on the corresponding value for Wyoming bentonite (85 meq/100g for a content of 75% montmorillonite). The mineral composition of Kunigel-V1 and the content of impurities are also listed in Table 7. The fact that distilled water was used in the experiments increases the significance of the impurities. The chemical composition of the porewater strongly depends on the degree of compaction and therefore affects the extent of Cs^+ sorption. The porosity values are obtained using $\rho_s = 2700$ kg/m^3 and $\varepsilon = 1 - (\rho_d/\rho_s)$, as reported by Sato et al. (1993). For the prediction of K_d we assume a CEC of 7.5 meq/100g for compacted Kunigel-V1 bentonite and that all the ion exchange sites are occupied with Na^+. Calculated K_d values are a factor of 3 higher, but the model correctly predicts the decrease in the K_d value with increasing degree of compaction.

Good agreement between the experimental and calculated K_d value is observed for the diffusion experiment conducted in a mixture of 10% Wyoming MX-80 bentonite and 90% silica with Allard water (Albinsson and Engkvist, 1991). This result is not in line with those obtained in batch-type experiments conducted in bentonite/sand mixtures, where the model underestimated the extent of Cs^+ sorption. This indicates that the model presented in this report provides reliable predictions for compacted bentonite as well as compacted bentonite/sand mixtures.

4 Testing the ion exchange model against miscellaneous diffusion and batch experiments from the literature

4.1 Testing against batch sorption experiments from the literature

The vast majority of batch sorption experiments of Cs^+ from the literature cannot be simulated with a predictive model, because the solid phases and the water compositions had not or insufficiently been characterised. In order to test our model, we can only use experiments for which sufficient information is provided on the type of solution used and the bentonite compo-

sition. Solubile impurities play an important role, especially if the solution is poorly mineralised. Table 10 presents a selection of published K_d values obtained from batch-type experiments for montmorillonite and for various bentonites.

For the study reported by Wahlberg and Fishman (1962) the model computations and the K_d values measured differ significantly. The simulation of the K_d values of these batch type experiments is of limited value because the compositions of the solid phases were not reported. For our simulations we assume that a Wyoming type montmorillonite (100% sodium form, CEC = 85 meq/100g) was used and that no impurities were present. The discrepancies between model and experiment are difficult to explain due to missing information about the materials used. It cannot be excluded that the discrepancies are due to uncertainities in the experimental results.

Mucciardi et al. (1978) carried out three experiments in different salt solutions of 0.03N each. In the model computations we assume that the montmorillonite used contained the same distribution of exchangeable ions and the same content of impurities as Wyoming bentonite MX-80 (Tables 1 or 7). The agreement between modelled and experimental K_d values is satisfactory.

The simulation of the K_d values of Wolfsberg (1978) is excellent, given the fact that again the bentonite impurities were not reported. We assume in our simulations that the chemical composition of the groundwater used by Wolfsberg (1978) corresponds to the chemical composition of Allard groundwater. The bentonite used in the experiment is assumed to be similar to Wyoming bentonite MX-80 (Tables 1 or 7).

The experiment of Erten et al. (1988) is simulated in the same manner. Allard groundwater is assumed to represent the chemical composition of the water type, and Wyoming MX-80 bentonite is assumed to represent the characteristics of the solid phase.

The simulation of the batch experiment of Miyahara et al. (1991) results in an almost identical K_d value as the one measured. The characteristic parameters for Kunipia-F bentonite slightly differ from those reported for Kunigel-V1 or Wyoming MX-80 bentonite. The impurities of Kunipia-F are 0.108% NaCl, 0.033% KCl and 1.02% $CaSO_4$ (Wanner and Wieland, 1993). The CEC of Kunipia-F bentonite is reported to 108 meq/100g with the following amounts of exchangeable ions: 97.1% Na, 0.93% K, 1.31% Ca and 0.65% Mg. Hence the proposed model for estimating Cs^+ sorption onto bentonite adequately predicts the K_d value for Kunipia-F bentonite (cf. Table 10).

4.2 Testing against diffusion experiments from the literature

Table 11 compares K_d values obtained from diffusion experiments, as reported in the open literature for bentonites other than Wyoming MX-80 and Kunigel-V1, with the values derived from the proposed model. The experiments listed in Table 11 comprise the diffusion experiments conducted by Cheung and Gray (1989) and Miyahara et al. (1991).

Table 10 Compilation of batch K_d values for Cs^+ in bentonite from different sources.

Solid phase	CEC [1] [meq/100g]	Solid/water ratio [g/cm³]	Water type	K_d(rep) [2] [m³/kg]	K_d(ix) [3] [m³/kg]	Ref. [4]
Montmorillonite No.11	n.r.	0.010	0.2M NaCl	0.8	0.180	1
	n.r.	0.010	0.2M KCl	0.2	0.106	
	n.r.	0.010	0.2M $MgCl_2$	1	0.036	
	n.r.	0.010	0.2M $CaCl_2$	0.9	0.034	
	n.r.	0.010	0.002M NaCl	20	4.01	
	n.r.	0.010	0.002M KCl	20	4.20	
	n.r.	0.010	0.002M $MgCl_2$	8	2.79	
	n.r	0.010	0.002M $CaCl_2$	4	2.55	
Montmorillonite No.21	n.r.	0.010	0.2M NaCl	0.3	0.180	1
	n.r.	0.010	0.2M KCl	0.2	0.106	
	n.r.	0.010	0.2M $MgCl_2$	0.2	0.036	
	n.r.	0.010	0.2M $CaCl_2$	0.3	0.034	
	n.r.	0.010	0.002M NaCl	10	4.01	
	n.r.	0.010	0.002M KCl	20	4.20	
	n.r.	0.010	0.002M $MgCl_2$	1	2.29	
	n.r.	0.010	0.002M $CaCl_2$	2	2.55	
Montmorillonite	87	0.033	0.03N $CaCl_2$	0.22	0.117	2
	87	0.033	0.03N $NaHCO_3$	1.56	0.919	
	87	0.033	0.03N NaCl	1.12	0.79	
Bentonite	72	0.05	nat. GW	1.57	1.75	3
	72	0.10	nat. GW	1.42	1.27	
Resadiye clay	n.r.	0.010	nat. GW [5]	3.5	2.75	4
Kunipia-F	108	0.001	distilled water	3.4	3.31	5

1) Cation exchange capacity, "n.r." = not reported.
2) K_d values reported by the authors.
3) K_d obtained from model computations using the ion exchange model
4) 1: Wahlberg and Fishman (1962), 2: Mucciardi et al. (1978), 3: Wolfsberg (1978), 4: Erten et al. (1988), 5: Miyahara et al. (1991).
5) Charge is not balanced in the composition of the groundwater reported.

Cheung and Gray (1989) used Avonlea clay, whose composition is not known. However, it is reported that Avonlea clay contains quartz sand. We assume that quartz sand is only present as trace impurity, and that hence the solid phase behaves like pure bentonite. Another very vague information is given about the type of water used in the experiments. We tentatively assign a specific composition to the terms "high salinity" and "low salinity" as used by Cheung and Gray (1989). In our model computations we assume that the chemical composition of the

Table 11 Compilation of apparent diffusivities for Cs^+ and derived K_d values in bentonite from different sources.

Solid phase	ρ_d [kg/m^3]	Water type	D_a [m^2/s]	K_d(rep)[1] [m^3/kg]	D_p [2] [m^2/s]	K_d [3] [m^3/kg]	K_d(ix) [4] [m^3/kg]	Ref. [5]
Avonlea clay [6]	1250	high salinity	4.5E-11 to 2.5E-10		6.2E-10	0.001 to 0.008	0.038	1
	1750	low salinity	2E-12		3.4E-10	0.034	0.051	
Kunipia-F	200	distilled water	1.5E-11	0.430	2.2E-9	0.680	0.954	2
	400		1.1E-11	0.158	1.7E-9	0.332	0.461	
	600		7.9E-12	0.098	1.4E-9	0.222	0.263	
	800		5.9E-12	0.057	1.1E-9	0.157	0.154	
	1000		4.4E-12	0.041	8.4E-10	0.120	0.136	
	1200		3.7E-12	0.025	6.6E-10	0.083	0.110	
	1400		2.2E-12	0.022	5.1E-10	0.080	0.080	
	1600		1.4E-12	0.018	4.1E-10	0.074	0.069	
	1800		7.9E-13	0.016	3.2E-10	0.074	0.035	
	2000		3.9E-13	0.016	2.5E-10	0.083	0.017	

1) K_d values reported by the authors as derived from the diffusivities.
2) Pore diffusivity, D_p, given as the diffusivity of HTO in Kunigel-V1 (Sato et al., 1993).
3) Calculated in this report from D_a and D_p.
4) K_d calculated in this report by using the ion exchange model developed in this report.
5) 1: Cheung and Gray (1989), 2: Miyahara et al. (1991).
6) For the calculation of D_p it is assumed that the solid behaves like pure bentonite with porosities of 50% for ρ_d = 1250 kg/m^3 and 35% for ρ_d = 1750 kg/m^3. "High salinity" is assumed to be represented by Äspö groundwater and "low salinity" by Allard groundwater.

highly saline water is represented by the chemical composition of Äspö water, and that the low salininity water is represented by the chemical composition of Allard groundwater. The experimental K_d values are estimated from the apparent diffusivity as measured by Cheung and Gray (1989) and the pore diffusivities as estimated in Section 3.2. Table 11 shows that the calculated K_d values are fairly close to the experimental values reported by Cheung and Gray (1989).

The experiments of Miyahara et al. (1991) were performed with Kunipia-F bentonite, which was reported to consist of >99% sodium montmorillonite. In the meantime, it has become known (Miyahara, 1993) that the amount of montmorillonite in Kunipia-F is >95% instead. The authors used distilled water for their diffusion experiments, which means that the aqueous phase provides no buffer capacity at all. Therefore, the results of the model calculations critically depend on the proportion of impurities present in the solid phase. The content of impurities in Kunipia-F has recently been determined to 0.108% NaCl, 0.033% KCl and 1.02% $CaSO_4$ (Wanner and Wieland, 1993). The CEC of Kunipia-F bentonite was reported to 108 meq/100g with the following amounts of exchangeable ions: 97.1% Na, 0.93% K, 1.31% Ca

and 0.65% Mg. The loss of available ion exchange sites due to the compaction of the bentonite is approached by assuming no loss up to a solid/water ratio of 0.5 g/ml (about ρ_d = 400 kg/m^3). The porosity values are calculated with Eq. (3). The CEC of highly compacted Kunipia-F bentonite (ρ_d = 2000 kg/m^3) is estimated to 13.5 meq/100g based on our findings that compaction causes a loss of available exchange by a factor of about 8 in Wyoming MX-80 bentonite (Section 3.3). A linear interpolation is used to calculate the CEC between ρ_d = 400 kg/m^3 (CEC = 108 meq/100g) and ρ_d = 2000 kg/m^3 (CEC = 13.5 meq/100g). The K_d values are recalculated from the experimentally determined diffusivities. We assume that the reference diffusivity measured in Kunigel-V1 by Sato et al. (1993) may also be used for Kunipia-F bentonite. Table 11 shows that the recalculated K_d values and those reported by Miyahara et al. (1991) differ by less than a factor of 4. Furthermore, good agreement is obtained between the recalculated K_d values and the ones predicted with the proposed ion exchange model.

In Figure 6 the predicted and experimental K_d values listed in Tables 10 and 11 are displayed. Figure 6 reveals that the ion exchange model developed in the present study can also be used to predict Cs^+ sorption for other experimental systems than those containing Wyoming MX-80 and Kunigel-V1 bentonite as the solid phase.

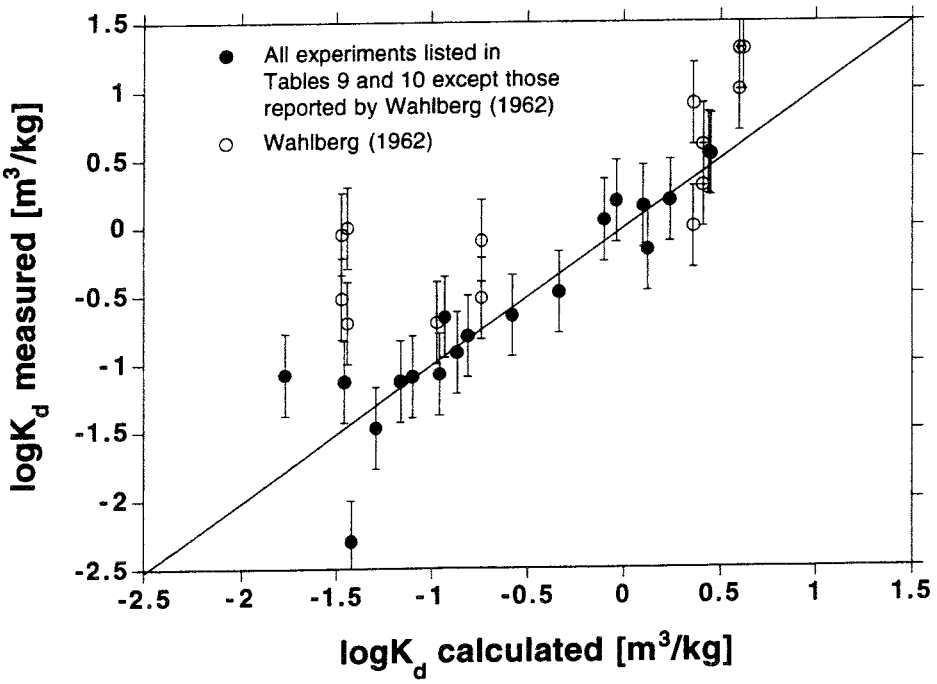

Figure 6 *Comparison of measured and calculated logK_d values for Cs^+ sorption evaluated from batch and diffusion experiments for the different clay minerals. The experimental conditions and references are listed in Tables 10 and 11. Uncertainties are estimated to ±0.3 in logK_d.*

5 Conclusions

The diffusion and sorption behaviour of caesium in bentonite and related clay minerals is described successfully by the use of a one-site ion exchange model. The ion exchange constant for Cs^+/Na^+ is derived from batch sorption experiments and determined to $\log K_{ex}^\circ = 1.6$. The diffusion experiments can be simulated with the same model by assuming that the cation exchange capacity (CEC) of compacted bentonite is reduced to about 12% of the total CEC of bentonite. In the diffusion model, the apparent diffusivity of tritiated water is used as the pore diffusivity of Cs^+, and the diffusion porosity is assumed to be equal to the bulk porosity. The errors made by these assumptions are implicitely contained in the reduction factor of the CEC.

The presented model for Cs sorption is tested against diffusion and batch-type measurements from different sources. Figure 7 shows that the predicted and measured values agree very well for most cases. More than 90% of the predictions are correct within an uncertainty range of ± 0.7 in $\log K_d$. Significant deviations are noted for 10/90 bentonite/sand mixtures with $McCl_2$ and $CaCl_2$ as background electrolyte. They may be due to experimental errors, i.e., difficulties arising when separating solid and supernatant at low suspension concentrations, or modelling errors, e.g., the mole fraction approach using a dependence of the ion exchange constants on the level of exchange, cf. Section 2.3.3. Significant deviations are also obtained for the experiments reported by Wahlberg and Fishman (1962).

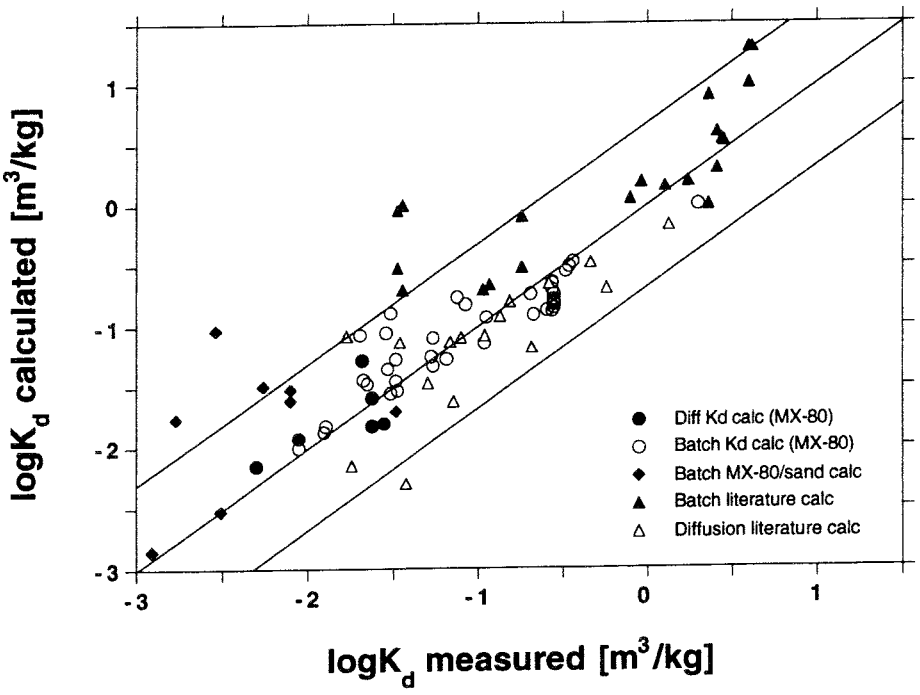

Figure 7 *Summary of all the data reported in Tables 5, 6, 9, 10 and 11. More than 90% of the data lie within the range of ± 0.7 in $\log K_d$ indicated by the two marginal lines.*

In addition, it is shown in this study that:

- distribution coefficients derived from both diffusion experiments and batch sorption experiments can be simulated by using a one-site ion exchange model.

- the ion exchange model correctly predicts the sorption curve of Cs^+ onto bentonite as a function of Cs^+ concentration between 10^{-9} M and 10^{-1} M Cs^+.

- the sorption behaviour of caesium on bentonites other than Wyoming MX-80 bentonite is reproduced equally well with the ion exchange model, provided that the composition of the solid phase is known.

- the soluble impurities that may be present in the solid phase can influence the sorption behaviour of caesium significantly, especially if the ionic strength of the groundwater is low.

- a 10/90 bentonite/silica sand mixture can be modelled as a "dilute" bentonite containing only 10% of the exchangeable ions of pure bentonite.

- with the aid of the ion exchange model, the distribution coefficient for Cs^+ can be predicted with an uncertainty of less than a factor of 3 for various bentonite/water systems and for a wide range of experimental conditions.

Uncertainties exist in two areas:

1. *Soluble impurities:* Reported compositions of bentonites usually consider the mineralogical composition only. However, natural bentonites always contain soluble salts as can be seen from the increasing concentrations of chloride, sulfate, nitrate, etc., in solutions after contact with bentonite. These impurities, which contain alkali and alkaline earth cations, compete with caesium for the ion exchange sites. Since most of these impurities have high solubilities, their concentrations in the solution in contact with the bentonite are determined by the solid/water ratio. It is, however, unclear what proportion of the soluble impurities can dissolve into the porewater of compacted bentonite. Since K_d is critically dependent on the amount of soluble impurities, especially in the case of weakly mineralised groundwaters, it is strongly recommended to analyse each type of bentonite in terms of its soluble impurities.

2. *Diffusion parameters:* The understanding of the migration behaviour of radionuclides in compacted bentonite depends on a realistic assessment of the diffusion parameters. Although the model presented in this report contains an internally consistent diffusivity data set, the available information is insufficient to determine the dependence of both the diffusion porosity and the available CEC on the compaction degree of bentonite. The problem is solved here by fixing the diffusion porosity at the level of the bulk porosity and to derive the available CEC. Although this procedure provides an internally consistent diffusivity data set, the parameters cannot be used with reliability for other radionuclides

because their diffusivities may depend on porosity and CEC in a different way than that of caesium. In the Appendix, possibilities to establish a consistent and realistic diffusivity database are discussed.

Keeping the potential sources for uncertainty in mind, the model presented in this report can be used to predict K_d values of caesium for a wide range of bentonite types and groundwater compositions. Table 12 presents a selection of predicted K_d values for Wyoming bentonite MX-80, a mixture of 10% MX-80 bentonite and 90% silica sand, as well as two Swedish reference groundwaters.

The direct use of the listed K_d values in diffusion models requires a check of the intrinsic parameters. In Table 12 the K_d values for compacted bentonite correspond to a dry density of $\rho_d = 2000$ kg/m^3 and a porosity of 0.3. Deviating parameters may lead to different K_d values. It is in any case safe to calculate K_d values by using the computer programme of the present model. This will allow an individual and correct assessment of the key parameters.

Table 12 K_d values predicted by the ion exchange model developed in the present report for a number of relevant near-field conditions, as well as for the corresponding batch type experiments.

Water type	Bentonite type	CEC [1] [meq/100 g]	Solid/water-ratio [g/cm^3]	Pore diffusivity, D_p [m^2/s]	K_d (Cs^+) [m^3/kg]
Allard [2]	MX-80	10	6.7 [4]	2.5×10^{-10} [4]	0.02 [5] 0.06 [6]
Allard [2]	10/90 MX-80/sand	1	6.7 [4]	2.5×10^{-10} [4]	0.005
Allard [2]	MX-80	85	0.01		2.0
Allard [2]	10/90 MX-80/sand	8.5	0.1		0.30
Äspö [3]	MX-80	10	6.7 [4]	2.5×10^{-10} [4]	0.009
Äspö [3]	10/90 MX-80/sand	1	6.7 [4]	2.5×10^{-10} [4]	0.001
Äspö [3]	MX-80	85	0.01		0.08
Äspö [3]	10/90 MX-80/sand	8.5	0.1		0.008

[1] Cation exchange capacity, depending on the compaction degree. This is the only parameter of the model that takes into account the reduction in available pore space in compacted bentonite, cf. Section 3.3.
[2] I = 0.004 M, composition listed in Table 2.
[3] I = 0.46 M, composition listed in Table 2.
[4] Corresponding to a dry density of $\rho_d = 2000$ kg/m^3 and a porosity of 0.3.
[5] Assuming that all soluble impurities (NaCl, $CaSO_4$, cf. Table 1) dissolve instantaneously in the porewater.
[6] Assuming that about 12% of the soluble impurities (proportional to the diminuation of the CEC in compacted bentonite) dissolve instantaneously in the porewater.

6 References

Albinsson, Y. (1993), Diffusion and sorption of Cs in bentonite/bentonite-sand mixtures, Internal Report KK930803, Chalmers University of Technology, Gothenburg, draft of August, 1993.

Albinsson, Y. (1993a), Personal communication to H.W., Dept. of Nuclear Chemistry, Chalmers University of Technology, Gothenburg, Sweden.

Albinsson, Y., Andersson, K., Börjesson, S. and Allard, B. (1993), Diffusion of radionuclides in concrete/bentonite systems, SKB TR 93-29.

Albinsson, Y. and Engkvist, I. (1991), Diffusion of Am, Pu, U, Np, Cs, I and Tc in compacted sand-bentonite mixture, Rad. Waste Manage. Nucl. Fuel Cycle, **15(4)**, 221-239.

Albinsson, Y., Forsyth, R., Skarnemark, G., Skålberg, M., Torstenfelt, B. and Werme, L. (1990), Leaching/migration of UO_2-fuel in compacted bentonite, Mat. Res. Soc. Symp. Proc., **176**, 559-565.

Brandberg, F. and Skagius, K. (1991), Porosity, sorption and diffusivity data compiled for the SKB 91 study, SKB TR 91-16.

Cheung, S.C.H. and Gray, M.N. (1989), Mechanism of ion diffusion in dense bentonite, Mat. Res. Soc. Symp. Proc., **127**, 677-681.

CRC Handbook of Chemistry and Physics (1990-1991), 71st ed. (D.R. Lide, Ed.), Boca Raton: CRC Press.

Erten, H.N., Aksoyoglu, S., Hatipoglu, S. and Göktürk, H. (1988), Sorption of caesium and strontium on montmorillonite and kaolinite, Radiochim. Acta, **44/45**, 147-151.

Fletcher, P. and Sposito, G. (1989). The chemical modelling of clay/electrolyte interactions for montmorillonite. Clay Minerals, **24**, 375 - 391.

Grenthe, I., Fuger, J., Konings, R.J.M., Lemire, R.J., Muller, A.B., Nguyen-Trung, C. and Wanner, H. (1992). Chemical thermodynamics of uranium (H. Wanner and I. Forest, Eds.), Amsterdam: North Holland.

Johnson, K.S. and Pytkowicz, R.M. (1978), Ion association with H^+, Na^+, K^+, Ca^{2+} and Mg^{2+} in aqueous solutions at 25°C. Amer. J. Sci., **278**, 1428-1447.

Miyahara, K. (1993), Personal communication to H.W., Power Reactor and Nuclear Fuel Development Corporation, Tokai-mura, Japan.

Miyahara, K., Ashida, T., Kohara, Y., Yusa, Y. and Sasaki, N. (1991), Effect of bulk density on diffusion for caesium, Radiochim. Acta, **52/53**, 293-297.

Mucciardi, A.N., Booker, I.J., Orr, E.C. and Cleveland, D. (1978), Statistical investigation of the mechanics controlling radionuclide sorption, in: WISAP Task 4, 2nd Contractor Meeting Proc., PNL-SA-7352.

Müller-Vonmoos, M. and Kahr, G. (1983), Mineralogische Untersuchungen von Wyoming-Bentonit MX-80 und Montigel, Nagra NTB 83-12, Baden, Switzerland.

Muurinen, A., Rantanen, J. and Penttilä-Hiltunen, P. (1986), Diffusion mechanisms of strontium, caesium and cobalt in compacted sodium bentonite, Mat. Res. Soc. Symp. Proc., **50**, 617-624.

Neretnieks, I. and Skagius, C. (1978), Diffusivity measurements of methane and hydrogen in wet compacted clay, KBS 86, in Swedish (Abstract in English).

Neretnieks, I. (1985), Diffusivities of some constituents in compacted bentonite clay and the impact on radionuclide migration in the buffer. Nucl. Technol., **71**, 458-470.

Sato, H., Ashida, T., Kohara, Y., Yui, M. and Sasaki, N. (1992), Effect of dry density on diffusion of some radionuclides in compacted sodium bentonite, J. Nucl. Sci. Technol., **29**, 873-882.

Sato, H., Ashida, T., Kohara, Y. and Yui, M. (1993), Study of retardation mechanism of ^{3}H, ^{99}Tc, ^{137}Cs, ^{237}Np and ^{243}Am in compacted sodium bentonite, Mat. Res. Soc. Symp. Proc., **294**, 403-408.

Snellman, M., Uotila, H. and Rantanen, J. (1987), Laboratory and modelling studies of sodium bentonite groundwater interaction, Mat. Res. Soc. Symp. Proc., **84**, 781-790.

Sposito, G. (1984), The surface chemistry of soils, New York: Oxford University Press.

Torstenfelt, B. (1986), Migration of the fission products strontium, technetium, iodine and cesium in clay, Radiochim. Acta, **39,** 97-104.

Torstenfelt, B. and Allard, B. (1986), Migration of fission products and actinides in compacted bentonite, SKB TR 86-14.

Torstenfelt, B., Allard, B., Andersson, K., Kipatsi, H., Eliasson, L., Olofsson, U. and Persson, H. (1983), Radionuclide diffusion and mobilities in compacted bentonite, KBS TR 83-34.

Wahlberg, J.S. and Fishman, M.J. (1962), Adsorption of caesium on clay minerals, Geol. Survey Bull., **1140-A**, A1-A30.

Wanner, H. (1986), Modelling interaction of deep groundwaters with bentonite and radionuclide speciation, Nagra NTB 86-21, Baden, Switzerland.

Wanner, H., Wersin, P. and Sierro, N. (1992), Thermodynamic modelling of bentonite-groundwater interaction and implications for near-field chemistry in a repository for spent fuel, SKB TR 92-37.

Wanner, H. and Wieland, E. (1993), Thermodynamic modelling of ion exchange reactions at the Na-smectite/water interface, PNC contract work, MBT Technical Report.

Wieland, E., Wanner, H., Albinsson, Y., Wersin, P. and Karnland, O. (1994). A surface chemical model of the bentonite/water interface and its implications for modelling the near-field chemistry in a reposiory for spent fuel. SKB Technical Report (in preparation).

Williams-Jones, A.E. and Seward, T.M. (1989), The stability of calcium chloride ion pairs in aqueous solutions at temperatures between 100 and 360°C, Geochim. Cosmochim. Acta, **53**, 313-318.

Wolfsberg, K. (1978), Sorption-desorption studies of Nevada Test Site. Alluvium and leaching studies of nuclear test debris, Los Alamos Scientific Laboratory, Informal Report LA-7216-MS, UC-11.

Appendix: Diffusivities and K_d's

A1 Discussion of factors influencing the diffusion behaviour of radionuclides

A1.1 Overview

Performance assessment for high-level nuclear waste disposal requires models that are capable to predict the migration behaviour of radionuclides in compacted bentonite. Diffusion measurements in compacted bentonite are a suitable laboratory method to simulate the migration behaviour of radionuclides in the near field of a high-level nuclear waste repository. The evaluation of the apparent diffusivity, D_a, from diffusion experiments has been described in several papers (e.g., Neretnieks, 1985; Torstenfelt, 1986) and is therefore not a subject of discussion here. The diffusivity of a radionuclide in an intact solid medium such as bentonite depends on a number of parameters describing the properties of the solid phase and the chemical interaction of the radionuclide with the solid:

$$R_D = \frac{D_p}{D_a} = 1 + \left(\frac{\rho_d}{\varepsilon}\right) K_d \tag{A1}$$

$$D_p = \frac{\delta}{\tau^2} D_v \tag{A2}$$

$$D_e = \varepsilon D_p \tag{A3}$$

$$\rho_d = (1 - \varepsilon)\, \rho_s \tag{A4}$$

$$\rho_w = \rho_d + \varepsilon \rho_f \tag{A5}$$

where

R_D	retardation factor
K_d	equilibrium distribution coefficient
D_a	apparent diffusivity [m^2/s]
D_p	pore diffusivity [m^2/s]
D_e	effective diffusivity [m^2/s]
D_v	diffusivity in the fluid [m^2/s]
ε	porosity of the solid
δ	constrictivity
τ^2	tortuosity
ρ_d	dry density of the solid [kg/m^3]
ρ_s	specific density of the solid [kg/m^3]
ρ_w	wet density (bulk density) of the solid [kg/m^3]
ρ_f	density of the pore fluid [kg/m^3]

Eq. (A1) relates the factor describing the chemical interactions, K_d, to the measured diffusivity, D_a. The pore diffusivity, D_p, represents the diffusivity of the radionuclide in the hypothetical case of zero adsorption and is therefore difficult to determine. Alternatively, if the

geometric factor δ/τ^2 is known, D_p can be derived according to Eq. (A2) from the diffusivity in the fluid, D_v. D_p can be determined by stationary diffusion measurements, cf. Eq. (A9). Eqs. (A3), (A4) and (A5) present relationships for the frequently used parameters D_e, ρ_s and ρ_w.

The prerequisite for reliable modelling of the migration behaviour of radionuclides in compacted bentonite is a consistent data set to solve Eq. (A1). A check of the variables contained in Eq. (A1) yields the following picture, e.g., for Cs^+:

D_p	not reliably known at present
D_a	known from various experimental determinations (e.g., Torstenfelt et al., 1983; Torstenfelt and Allard, 1986; Albinsson and Engkvist, 1991; Albinsson, 1993; Albinsson et al., 1993)
ρ_d	known for a given solid phase and compaction level
ε	known for a given solid phase and compaction level, although the porosity which is effectively available for diffusion, is probably considerably lower
K_d	batch K_d values cannot be directly used in Eq. (A1)

Consequently, the parameters that require more detailed consideration are D_p, ε and K_d. They are further discussed in the following paragraphs.

A1.2 The pore diffusivity, D_p

The pore diffusivity, D_p, represents the diffusion of a radionuclide in the hypothetical case of no chemical adsorption. Hence, the difference between D_a and D_p is, in principle, entirely due to chemical sorption, denoted K_d, at a given ratio of solid to fluid (ρ_d/ε). The factors listed below can influence D_p.

- The mobility of the radionuclide, which is a function of the size of the diffusing species, has an effect on its diffusivity, although this effect may in many cases be small compared to the uncertainties. A direct measure of the mobility of an ion is its ionic conductivity. For simple ions, values of the ionic conductivities are tabulated in the CRC Handbook of Chemistry and Physics (1990-1991). For example, the ionic conductivity at infinite dilution of caesium is $\Lambda_0(Cs^+) = 77.2$ cm^2S/mol, and that of strontium is $\Lambda_0(Sr^{2+}) = 118.8$ cm^2S/mol. The pore diffusivities of Cs^+ and Sr^{2+} may be considered to relate to each other like the equivalent ionic conductivities:

$$\frac{D_p(Cs^+)}{D_p(Sr^{2+})} = \frac{\Lambda_0(Cs^+)}{\frac{1}{2}\Lambda_0(Sr^{2+})} = \frac{77.2}{59.4} = 1.3 \qquad \text{(A6)}$$

  This relationship appears applicable if other effects (see following items) can be excluded. However, care has to be taken when adopting ionic condictivity values from general tabulations such as the CRC Handbook of Chemistry and Physics (1990-1991). For

example, in that table the ionic conductivity of the uranyl ion, $\Lambda_0(UO_2^{2+})$ = 64 cm^2S/mol, seems very low for a +2 ion. Since hydrolysis of UO_2^{2+} begins above a pH of 5, it is probable that the uranium was actually present as a mixture of UO_2^{2+} and $UO_2(OH)_2$ during the conductivity measurement, cf. Grenthe et al. (1992). It should be mentioned that some authors have tried to express the mobility of an ion as a function of its ionic radius, e.g., Albinsson and Engkvist (1991). This procedure becomes very complex for nuclides that are present in different chemical forms in solution. Furthermore, it should be noted that the radii of the dissolved and hydrated species are not correctly represented by the ionic radii as obtained from crystallographic analysis.

- The mobility effect described in the item above may in certain cases be dominated by a charge effect. Since surfaces, especially in clay minerals, carry a fixed negative surface charge (cation exchange sites), the diffusion without sorption of an anion may differ from that of a cation due to electrostatic effects, even if their ionic conductivities are the same. It is therefore difficult to compare pore diffusivities of oppositely charged ions, and it is not advisable to use analogue relationships to derive cation D_p's from anion D_p's and vice versa.

- There may be other effects that influence the pore diffusivities in different ways for different diffusing species. Neretnieks and Skagius (1978) measured the diffusivities of dissolved methane and hydrogen gas in compacted bentonite by stationary diffusion experiments (cf. Section A2.2). Although $H_2(aq)$ is smaller than $CH_4(aq)$ and therefore more mobile in aqueous solution, it diffuses more slowly than $CH_4(aq)$: $D_p(H_2, aq) = 1.8\times10^{-11}$ m^2/s and $D_p(CH_4, aq) = 3.9\times10^{-11}$ m^2/s. A plausible explanation is that even small pores, including dead-end pores, are available for $H_2(aq)$ while they are not available for $CH_4(aq)$, and the dispersion of $H_2(aq)$ may thus be more extensive, leading to a larger retardation of $H_2(aq)$.

It is therefore obvious that D_p is a nuclide specific parameter. Using the same value of D_p for a variety of radionuclides, as has been done to a large extent by Brandberg and Skagius (1991), may sometimes be unavoidable, but one has to be aware that this procedure may lead to inconsistencies and errors in predictions of the migration behaviour.

Estimations of D_p by analogy with chemically unretarded species should be corrected for the effects mentioned above, as far as this is possible. Several tracers have been suggested as reference species to estimate D_p, because they are considered to undergo no chemical reactions with the bentonite surface: Cl^-, I^-, HS^-, TcO_4^-, $CH_4(aq)$ and tritiated water, HTO. However, considering the factors that may influence D_p as mentioned above, the assumption that D_a values of these species can be used to represent unretarded diffusion of positively charged radionuclides is affected with uncertainties that are difficult to quantify.

A1.3 The porosity, ε

The porosity contained in Eqs. (A4) and (A5) refers to the total porosity of the bentonite. However, in compacted bentonite only a fraction of the total pore size is expected to be available for diffusion. The high densities lead to a compression of the pores in such a way that some of them may become too narrow for many solute species. The effective porosity available for diffusion, as used in Eqs. (A1) and (A3), will thus most probably not be equal to the total porosity of Eqs. (A4) and (A5). Unfortunately, reliable assessments of the pore size reduction due to compaction are not available to date. Diffusion measurements as a function of the compaction degree have been reported by Miyahara et al. (1991) and Sato et al. (1992, 1993), but it is not yet clear what proportion of the change in the apparent diffusivity is due to a change in the available porosity. As mentioned in the paragraph above, charge and size effects may play a significant role, and the available porosity may thus differ according to the kind of radionuclide.

At present, any predictions about the change in available porosity seem speculative. It may therefore be acceptable to use the total porosity, ε, in all the calculations, cf. Brandberg and Skagius (1991). The error made by this simplification is then included in other variables.

A1.4 The equilibrium distribution coefficient, K_d

K_d is defined as the ratio of radionuclide, M, sorbed on the surface of the solid to radionuclide in solution:

$$K_d = \frac{[M]_{sorbed} \quad [mol/kg]}{[M]_{dissolved} \quad [mol/m^3]} \tag{A7}$$

K_d is thus customarily defined as a bulk parameter because it does not distinguish between different chemical forms of the radionuclide on the surface and in the solution. However, K_d can also be expressed on a thermodynamic basis:

$$K_d = \frac{\sum_j \{MX_j\} \quad [mol/kg]}{\sum_m \sum_{q_1} \sum_{q_2} \ldots \left(m\, \beta_{m,q_1,q_2,\ldots} [M]^m [L_1]^{q_1} [L_2]^{q_2} \ldots\right) \quad [mol/m^3]} \tag{A8}$$

This means that K_d can be predicted if both the surface speciation (numerator) and the solution speciation (denominator) of M in a given system are known.

K_d values are preferably determined by using batch techniques and by taking comparatively small amounts of solid. In this way, physical heterogeneities that may arise from compacting the solid can be excluded, the surface properties can be investigated by well-known methods, and equilibrium between the aqueous radionuclide and its sorbed form can be expected to establish within experimental timeframes.

However, the chemical conditions in a batch experiment, in which small amounts of bentonite are equilibrated with comparatively large quantities of solution, are usually considerably different from those in diffusion experiments by which the situation in compacted bentonite is simulated, cf. Wieland et al. (1994). It is therefore not surprising that radionuclide distribution coefficients, K_d values, cannot be the same under such different conditions. However, the surface interaction processes, which can be described by thermodynamic models, can be expected to be the same under a large variety of conditions, at least for radionuclides with simple interaction mechanisms. It is possible that some radionuclides, especially those whose solution chemistry is complex and which may be present in different chemical forms in solution, may interact with the solid surface by several mechanisms and form different surface complexes under different chemical conditions. However, Cs^+ for example is known to participate in ion exchange processes, and it is highly probable that the adsorbed form of Cs^+ is the same at any compaction degree of the solid.

The determination of K_d from diffusion experiments is not straightforward due to the uncertainties in determining D_p and ε, cf. Sections A1.2 and A1.3 above. Albinsson and Engkvist (1991) have derived "diffusion K_d's" by assuming that D_p is based on the apparent diffusivity of TcO_4^-, corrected for differences in the crystalline radii, and that ε represents the total porosity of the compacted solid. Uncertainties and deviations in D_p and ε are therefore cumulated in the calculated K_d values. On the other hand, Neretnieks (1985) used batch K_d values in the interpretation of diffusion experiments and found that the resulting values of D_p or ε did not match with the expectations.

In summary, it appears crucial that surface interaction mechanisms are considered for the derivation of K_d, as is shown in Eq. (A8), rather than relying on bulk determinations according to Eq. (A7).

A2 Procedures for establishing data sets of D_p, ε and K_d for bentonite

A reliable diffusivity data base contains a consistent set of D_p, ε and K_d for each radionuclide. Neretnieks (1985) found that the use of K_d values from batch experiments leads to D_p and ε values that are incompatible with the expectations. As mentioned in Section A1.4 above, K_d values measured by batch techniques are not applicable to compacted bentonite due to differences in the chemical conditions. However, measurements at low solid/liquid ratios provide the basis for the development of mechanistic models, such as surface complexation and ion exchange models.

K_d values are thus determined separately, i.e., by batch type sorption experiments, and the sorption models must be checked for their applicability in compacted bentonite. Their application to compacted bentonite requires the knowledge of the amount of available surface sites and is therefore directly linked to the effective diffusion porosity, ε. However, it may be possibile to establish a consistent set of D_p, ε and K_d values for simple tracers if the D_p value

can be determined independently. The following sections discuss possible ways to determine pore diffusivities.

A2.1 Estimations of pore diffusivities, D_p

D_p values for radionuclides may be estimated based on analogies, and by taking into account correction factors due to

- differences in the mobilities of the diffusing species
- charge effects (ion exclusion)
- differences in the sizes of the diffusing species

as outlined in Section A1.2 above. Such estimations need to be verified independently, for example by using K_d values that are based on mechanistic models. This seems feasible for simple radionuclides such as Cs^+, Sr^{2+} or TcO_4^-.

A2.2 Measurement of D_p by stationary diffusion experiments

Diffusion experiments can be carried out by a stationary technique (cf., e.g., Neretnieks and Skagius, 1978; Neretnieks, 1985), in contrast to the non-stationary experiments usually used for radionuclide diffusion measurements through compacted bentonite (cf., e.g., Albinsson et al., 1990; Albinsson and Engkvist, 1991; Albinsson et al., 1993). In the stationary diffusion experiments, a constant flux, N, of the tracer is reached after a certain time. N can then be used to determine the pore diffusivity, D_p:

$$N = D_p \varepsilon A \frac{dc}{dx} \tag{A9}$$

where (ε A) is the surface area available for diffusion and (dc/dx) the concentration gradient. This method leads to an equilibrium saturation of the surface sites for retarded radionuclides. When the sorbed radionuclide is in equilibrium with the one in solution over the whole diffusion length, then the flux, N, will become constant and will be determined by the pore diffusivity of the radionuclide, because no net retardation will occur at this stage. The equilibration time required may be too long for strongly retarded nuclides to use this technique to determine D_p. However, the direct determination of D_p appears like a promising tool in establishing and verifying a consistent data base of D_p, ε and K_d values.

It should be mentioned that by flushing the diffusion cell, dissolved ions of the bentonite pore water will be flushed away in addition to the tracer. These ions should be replaced at the inflow of the diffusion cell to avoid leaching of the bentonite which would alter the chemical conditions. It is recommended to use tracer dissolved in (synthetic) equilibrium bentonite pore water to avoid leaching.

A2.3 Derivation of D_p from diffusivities in the fluid, D_v

According to Eq. (A2) it is possible, in principle, to derive D_p from tabulated D_v values, cf. the CRC Handbook of Chemistry and Physics (1990-1991), if the factor δ/τ^2 is known. Although a direct derivation of the factor δ/τ^2 seems possible for supposedly unretarded radionuclides (for which $D_p = D_a$), or for retarded radionuclides if D_p can be measured directly through stationary diffusion experiments (cf. Section A2.2 above), this procedure presents no advantage compared to Eq. (A6) which relates the D_p values to the ionic conductivities. Neretnieks (1985) stated that "the geometric factor δ/τ^2 is not constant", meaning that this factor is not only dependent on the kind and state of the solid medium, but also on the kind of radionuclide and its chemical speciation. In this respect, the comments presented in Section A1.2 apply here as well.

A2.4 Dependence of D_p on the compaction level of bentonite

Diffusion experiments reported in the literature do not always refer to the same compaction level of bentonite. The compaction level is best represented by either the dry density, ρ_d, or the bulk density, ρ_w, cf. Eqs. (A4) and (A5). We may assume that the diffusivity measurements of tritiated water, HTO, performed by Sato et al. (1993) at different dry density values reflect the dependence of D_p on the dry density of bentonite. We may also assume that this dependence, measured on Kunigel-V1 (a Na-bentonite reported to contain 50-55% Na-montmorillonite), applies also to Wyoming bentonite MX-80. These assumptions are based on the chemically unretarded diffusion behaviour of HTO, cf. Figure 4 of Sato et al. (1993). An unweighted linear regression of $\log_{10}D_a$(HTO) vs. ρ_d, cf. Figure A1, yields the following result:

$$\log_{10}D_a(\text{HTO}) = -5.24\times10^{-4}\,\rho_d - 8.554. \qquad \text{(A10)}$$

Units are [kg m^{-3}] for ρ_d and [m^2s^{-1}] for D_a. From Figure 4 of Sato et al. (1993) it can be seen that this approach is reasonable for caesium as the slope of the curves for ^3H and ^{137}Cs are very similar. However, the figure also shows that for other radionuclides the dependence of D_a on the compaction level of bentonite may have different slopes; non-linearity is also fairly common, cf. Figure 4 of Sato et al. (1992) for Kunipia-F bentonite (>95% Na-montmorillonite).

The resulting intersection at $\rho_d = 0$, cf. Eq. (A10), may be interpreted as the diffusivity of HTO in pure water, D_v(HTO). From Eq. (2) the geometric factor δ/τ^2 can then be calculated if we assume that HTO is not chemically retarded in bentonite (i.e., if $D_p = D_a$). In the present case for Kunigel-V1 bentonite, we obtain $\log_{10}D_v(\text{HTO}, \rho_d = 0) = 2.8\times10^{-9}$ m^2/s. As a comparison, Sato et al. (1992) reported a diffusivity of H_2O in free water as $\log_{10}D_v(H_2O$, in water$) = 2.3\times10^{-9}$ m^2/s, which is not incompatible with the value for HTO obtained here. From our value of D_v for HTO, by assuming that D_p(HTO) = D_a(HTO), and by applying Eqs. (A2) and (A10) we obtain $\delta/\tau^2 = 0.090$ at $\rho_d = 2000$ kg/m^3.

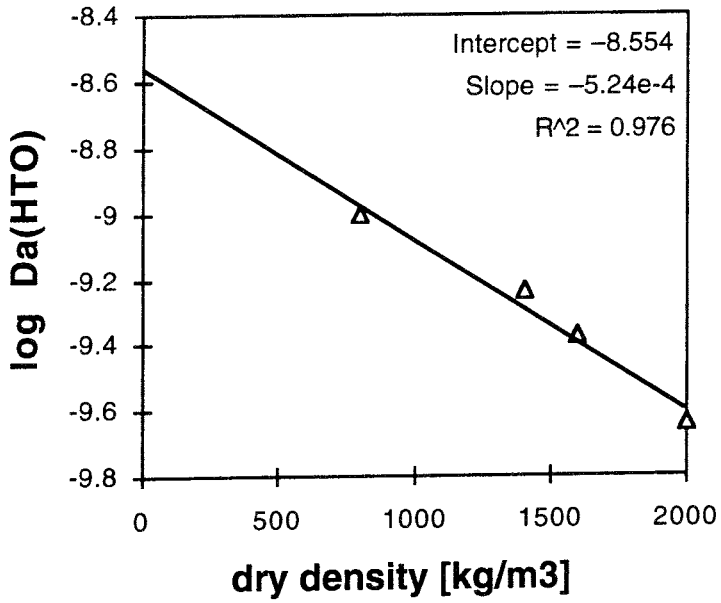

Figure A1: Linear regression of the apparent diffusivities, $log_{10}D_a$, of tritiated water, HTO, as a function of the dry density of Kunigel-V1 bentonite. The data are from Sato et al. (1993).

This simple evaluation shows that diffusion measurements at different compaction levels represent a useful tool to verify mechanistic diffusion models.

A3 Summary and recommendations

In this Appendix the parameters required to establish a consistent diffusivity data base for radionuclides are discussed. The critical parameters are the pore diffusivity, D_p, i.e., the diffusivity in the hypothetical case of zero adsorption, the porosity, ε, and the distribution coefficient, K_d. Problems arise due to the fact that the pore diffusivities vary from one radionuclide to the other, and that in some cases even the available diffusion porosity may depend on the type of radionuclide. The following items need to be considered when developing a diffusivity data base:

- Pore diffusivities, D_p, depend on the mobility of the radionuclide, on the chemical conditions in the pore system, i.e., the speciation of the radionuclide, on the charge of the radionuclide, and on its size. Independent measurements of D_p are, in principle, possible with stationary diffusion experiments.

- Porosities, ε, as obtained by Eq. (A4), represent the total pore space of the compacted bentonite. However, only a part of the pore space may be available for diffusion, and a

reduction factor should therefore be determined. It is important to note that the reduction factor has an impact on the determination of K_d, because it is a measure for the proportion of available surface sites for sorption. The consistent pair of K_d and ε values has to be determined by iteration.

- The distribution coefficient, K_d, measured by batch techniques, cannot be directly used in Eq. (A1), because the determining chemical environment in compacted bentonite is distinctly different from that at low solid/liquid ratios. Since diffusion measurements, whose primary goal is to determine apparent diffusivities, D_a, already involve a couple of uncertain parameters (D_p and ε), they are not suitable to determine reliable K_d values. It is therefore necessary to develop thermodynamic interaction models that account for the chemical differences between batch experiments and compacted bentonite.

It is suggested to start with a simple system to determine the parameters D_p and ε, in parallel with K_d. Direct determination of D_p is recommended in cases where this is feasible (weak and medium retardation). With the help of a thermodynamic sorption model it will then be possible to evaluate the effective porosity by iteration. Such a data set may form the basis for further evaluations for more complex radionuclides. In this way, it may sometimes suffice to apply correction factors to account for differences in the radionuclide behaviour.

A special problem that we have to face is the difficulty in predicting the redox conditions in compacted bentonite. Redox sensitive elements, such as technetium, uranium or neptunium, exhibit extremely different migration behaviour at different oxidation states. Parameter variations in the thermodynamic models may give an indication of the magnitude of the redox effects.

List of SKB reports

Annual Reports

1977-78
TR 121
KBS Technical Reports 1 – 120
Summaries
Stockholm, May 1979

1979
TR 79-28
The KBS Annual Report 1979
KBS Technical Reports 79-01 – 79-27
Summaries
Stockholm, March 1980

1980
TR 80-26
The KBS Annual Report 1980
KBS Technical Reports 80-01 – 80-25
Summaries
Stockholm, March 1981

1981
TR 81-17
The KBS Annual Report 1981
KBS Technical Reports 81-01 – 81-16
Summaries
Stockholm, April 1982

1982
TR 82-28
The KBS Annual Report 1982
KBS Technical Reports 82-01 – 82-27
Summaries
Stockholm, July 1983

1983
TR 83-77
The KBS Annual Report 1983
KBS Technical Reports 83-01 – 83-76
Summaries
Stockholm, June 1984

1984
TR 85-01
Annual Research and Development Report 1984
Including Summaries of Technical Reports Issued during 1984. (Technical Reports 84-01 – 84-19)
Stockholm, June 1985

1985
TR 85-20
Annual Research and Development Report 1985
Including Summaries of Technical Reports Issued during 1985. (Technical Reports 85-01 – 85-19)
Stockholm, May 1986

1986
TR 86-31
SKB Annual Report 1986
Including Summaries of Technical Reports Issued during 1986
Stockholm, May 1987

1987
TR 87-33
SKB Annual Report 1987
Including Summaries of Technical Reports Issued during 1987
Stockholm, May 1988

1988
TR 88-32
SKB Annual Report 1988
Including Summaries of Technical Reports Issued during 1988
Stockholm, May 1989

1989
TR 89-40
SKB Annual Report 1989
Including Summaries of Technical Reports Issued during 1989
Stockholm, May 1990

1990
TR 90-46
SKB Annual Report 1990
Including Summaries of Technical Reports Issued during 1990
Stockholm, May 1991

1991
TR 91-64
SKB Annual Report 1991
Including Summaries of Technical Reports Issued during 1991
Stockholm, April 1992

1992
TR 92-46
SKB Annual Report 1992
Including Summaries of Technical Reports Issued during 1992
Stockholm, May 1993

Technical Reports
List of SKB Technical Reports 1994

TR 94-01
Anaerobic oxidation of carbon steel in granitic groundwaters: A review of the relevant literature
N Platts, D J Blackwood, C C Naish
AEA Technology, UK
February 1994

TR 94-02
Time evolution of dissolved oxygen and redox conditions in a HLW repository
Paul Wersin, Kastriot Spahiu, Jordi Bruno
MBT Technología Ambiental, Cerdanyola, Spain
February 1994

TR 94-03
Reassessment of seismic reflection data from the Finnsjön study site and prospectives for future surveys
Calin Cosma[1], Christopher Juhlin[2], Olle Olsson[3]
[1] Vibrometric Oy, Helsinki, Finland
[2] Section for Solid Earth Physics, Department of Geophysics, Uppsala University, Sweden
[3] Conterra AB, Uppsala, Sweden
February 1994

TR 94-04
Final report of the AECL/SKB Cigar Lake Analog Study
Jan Cramer (ed.)[1], John Smellie (ed.)[2]
[1] AECL, Canada
[2] Conterra AB, Uppsala, Sweden
May 1994

TR 94-05
Tectonic regimes in the Baltic Shield during the last 1200 Ma - A review
Sven Åke Larsson[1,2], Eva-Lena Tullborg[2]
[1] Department of Geology, Chalmers University of Technology/Göteborg University
[2] Terralogica AB
November 1993

TR 94-06
First workshop on design and construction of deep repositories - Theme: Excavation through water-conducting major fracture zones Såstaholm Sweden, March 30-31 1993
Göran Bäckblom (ed.), Christer Svemar (ed.)
Swedish Nuclear Fuel & Waste Management Co, SKB
January 1994

TR 94-07
INTRAVAL Working Group 2 summary report on Phase 2 analysis of the Finnsjön test case
Peter Andersson (ed.)[1], Anders Winberg (ed.)[2]
[1] GEOSIGMA, Uppsala, Sweden
[2] Conterra, Göteborg, Sweden
January 1994

TR 94-08
The structure of conceptual models with application to the Äspö HRL Project
Olle Olsson[1], Göran Bäckblom[2], Gunnar Gustafson[3], Ingvar Rhén[4], Roy Stanfors[5], Peter Wikberg[2]
1 Conterra AB
2 SKB
3 CTH
4 VBB/VIAK
5 RS Consulting
May 1994

TR 94-09
Tectonic framework of the Hanö Bay area, southern Baltic Sea
Kjell O Wannäs, Tom Flodén
Institutionen för geologi och geokemi, Stockholms universitet
June 1994